Energy 321 (2025) 135221

Contents lists available at ScienceDirect

Energy

journal homepage: www.elsevier.com/locate/energy

A novel production cost model for provision of capacity firming by prosumer batteries

Mohsen Aldaadi [a,b,1], Miloš Pantoš [c,1], Shariq Riaz [d], Archie C. Chapman [e], Gregor Verbič [a,*]

[a] School of Electrical and Computer Engineering, The University of Sydney, Australia
[b] School of Electrical Engineering, Islamic University of Madinah, Madinah, Saudi Arabia
[c] Faculty of Electrical Engineering, University of Ljubljana, Slovenia
[d] KPMG, Sydney, Australia
[e] School of Information Technology and Electrical Engineering, The University of Queensland, Brisbane, Australia

ARTICLE INFO

Keywords:
Renewable energy
Battery storage
Capacity firming
Prosumers
Virtual power plants
Bilevel optimization

ABSTRACT

The increasing integration of variable renewable energy sources requires firming resources, typically involving storage, gas generation, and new transmission infrastructure to maintain a reliable power supply. In contrast, this paper argues that using prosumer-owned batteries coupled with rooftop solar systems is a promising alternative. A production cost model is proposed to study the provision of capacity-firming services by prosumer virtual power plants in future grid scenario analysis. The model employs a bilevel optimization framework that (1) enables prosumers to prioritize self-consumption before offering surplus battery capacity for firming services, ensuring operational autonomy, and (2) allows the system operator to select the most cost-effective prosumer solutions without compromising the overall benefits to prosumers. The model effectiveness is evaluated through a case study of the Australian National Electricity Market. Results indicate that prosumer-owned batteries can significantly lower the cost of capacity firming by reducing reliance on gas generation and utility-scale storage. Furthermore, capacity-firming services provide prosumers with an additional revenue stream, enhancing the economic viability of home batteries. However, the study also reveals a decreasing marginal benefit of the value of the capacity-firming service provided by prosumers as their battery size relative to solar capacity increases.

1. Introduction

Electric power systems around the world are undergoing a massive transition driven by efforts to decarbonize the economy [1]. In Australia, the transformation is remarkably rapid—due to the ever-decreasing cost of renewable generation, coupled with the excellent availability of wind and solar resources and abundant land, all coal-fired generation will close by 2038, if not sooner, as stated in the Australian Integrated System Plan [2]. Replacing conventional fossil fuel generation with variable renewables is challenging. Ensuring that sufficient supply is available to meet the demand at all times requires additional transmission infrastructure to increase the geographic diversity of renewables and firming resources to cater for still cloudy periods. The firming capacity can come from various storage technologies and gas generation. Although these technologies are well understood, they are costly and often challenging to install.

1.1. Motivation

Another alternative is utilizing the flexibility of distributed energy resources (DERs) located 'behind the meter' in residential and small commercial buildings—an often overlooked option [3]. These DERs transform traditional consumers into prosumers who actively produce, consume, and manage their energy. In response to signals such as energy prices, grid reliability, carbon intensity, or renewable energy availability, prosumers can adjust their energy consumption—a capability known as demand flexibility [4]. Demand flexibility is becoming increasingly important as the energy industry transitions to a more distributed, renewable, and decarbonized energy system, complementing 'conventional' flexible options, such as energy storage [5]. By enabling prosumers to actively manage their energy use, demand flexibility can help balance the grid, reduce the need for a new energy infrastructure, and reduce carbon emissions. It can also provide cost savings for

* Corresponding author.
E-mail addresses: mohsen.aldaadi@sydney.edu.au, maldaadi@iu.edu.sa (M. Aldaadi), milos.pantos@fe.uni-lj.si (M. Pantoš), sriaz3@kpmg.com.au (S. Riaz), archie.chapman@uq.edu.au (A.C. Chapman), gregor.verbic@sydney.edu.au (G. Verbič).
[1] Joint first authors.

https://doi.org/10.1016/j.energy.2025.135221
Received 6 December 2024; Received in revised form 17 February 2025; Accepted 21 February 2025
Available online 6 March 2025
0360-5442/

Nomenclature

Abbreviations

DER	Distributed energy resource
FC	Firm capacity
MPEC	Mathematical program with equilibrium constraints
KKT	Karush–Kuhn–Tucker optimality conditions
PV	Photovoltaic
RES	Renewable energy source
SOC	State of charge
VPP	Virtual power plant
LL	Lower level
UL	Upper level

Sets and indices

$t \in \mathcal{T}$	Set of time slots t
$g \in \mathcal{G}$	Set of generators g
$s \in \mathcal{S}$	Set of utility-scale batteries s
$c \in \mathcal{C}$	Set of consumers c
$p \in \mathcal{P}$	Set of prosumer VPPs p
$l \in \mathcal{L}$	Set of transmission lines l
$n \in \mathcal{N}$	Set of nodes n

Variables

$o \in \mathbb{Z}_{\geq 0}$	Number of online units
$u \in \mathbb{Z}_{\geq 0}$	Start-up status
$d \in \mathbb{Z}_{\geq 0}$	Shut-down status
$p \in \mathbb{R}$	Active power
$e \in \mathbb{R}$	Energy state of charge
$\Psi \in \{0, 1\}$	Battery charging status
$r \in [0, 1]$	Battery charging rate (fraction of capacity)

Superscripts (descriptors)

FC	Firm capacity
fix	Fixed
su	Start-up
sd	Shut-down
var	Variable
gas	Gas-fired power plants
syn	Synchronous
B	Utility-scale battery
b	Prosumer VPP battery
d	Demand
g	Grid
rsv	Reserve
pen	Penalty

Constants and parameters

c	Cost
FC	Required firm capacity
LF	System losses factor
τ	Minimum time
U	Number of identical units
η	Battery efficiency
r	Ramp-rate.
B	Transmission line susceptance
P	Power demand
Δt	Time resolution

Notation

$\bullet^{+/-}$	Up/down, charge/discharge, from/to the grid
$\hat{\bullet}$	Initial value
$\underline{\bullet}/\overline{\bullet}$	Minimum/maximum value

Example

$p^{\text{b,FC}-}_{p,t}$	Firm capacity battery discharge power of prosumer VPP p in time slot t

customers who can take advantage of lower prices during off-peak hours and potentially generate revenue through participation in demand response programs, including virtual power plants (VPPs).

Using demand flexibility as a valuable system resource is particularly attractive in countries with a high penetration of DER, such as Australia, where policy frameworks and market reforms are actively evolving to facilitate greater prosumer participation, as highlighted by reports from the Energy Security Board (ESB) [6,7]. For example, the penetration of residential rooftop solar photovoltaic (PV) and home batteries in the National Electricity Market (the interconnection spanning the eastern Australian seaboard) is predicted to increase to 50 GW and 40 GWh, respectively, by 2050 [8][2]; this offers an unprecedented opportunity to use these resources to firm variable renewables. This value has been acknowledged by governments and market-making bodies, including by the Australian government which aims to introduce auction mechanisms for procuring firming capacity to support variable renewable generation, with explicit mention of the potential firming value of aggregated DER and VPPs.[3] Residential solar-battery systems are particularly attractive for two reasons: first, they are a consumer-financed resource, so using them for capacity firming does not increase the social cost[4]; and second, they are installed in residential buildings with less onerous connection requirements compared to utility-scale resources. However, private ownership also prevents the system operator from directly controlling the home battery systems. The primary purpose of home batteries is to reduce the owner's energy expenditure and not to participate in system operation directly. In other words, prosumers pursue their private objective that might not align with the objective of the system operator.

While existing studies have predominantly focused on centralized, supply-side firming solutions, limited attention has been given to the potential of prosumer-owned batteries as a decentralized, cost-effective alternative. Current approaches to demand flexibility typically assume a unidirectional flow with full control by the system operator, often overlooking the challenges associated with prosumers' private ownership and their usage priorities.

This challenge is addressed by proposing a *production cost model* for future grid scenario analysis, evaluating the potential of prosumer-owned batteries for capacity firming. The conflict arising from private ownership is reconciled by formulating the problem as a bilevel optimization model, where the upper level represents the system operator minimizing generation costs, while the lower level represents prosumers maximizing rooftop solar self-consumption.[5] The excess capacity of the home battery is then offered to the system operator for capacity firming.

[2] For comparison, the total utility-scale generation, distributed solar and home battery capacity in 2022 was 65 GW, 14 GW and 2.7 GWh, respectively.

[3] www.dcceew.gov.au/energy/renewable/capacity-investment-scheme.

[4] This excludes government subsidies aiming to boost the adoption of DERs that still exist in many jurisdictions.

1.2. Related work

To maintain the reliability of the network, the electricity supply must always match the demand. However, renewable energy sources (RES), such as wind and solar, are variable and their output can change rapidly depending on weather conditions. The National Renewable Energy Laboratory (NREL) conducted one of the first studies on the need for *grid flexibility* focusing on energy storage [5]. Although they did not use that term, they were the first to propose what is now called *capacity firming*, which refers to the process of maintaining a consistent and reliable amount of power from an intermittent source to meet demand or to compensate when renewable sources do not produce enough electricity. Capacity firming can be achieved by energy storage, such as batteries or pumped hydro, and dispatchable generators, such as gas-fired power plants.

Different aspects of the capacity firming problem have been addressed in the existing literature. The impact of energy droughts on firm capacity requirements has been analyzed using fuel-based technologies, such as hydrogen [9]. The effectiveness of open-cycle gas turbines and battery storage as firming solutions for merchant wind farms has been evaluated [10]. The use of battery storage combined with deep-learning irradiance forecasting has been examined to enhance the dispatchability of large solar PV plants with minimized storage capacity [11]. A probabilistic optimization strategy has been proposed to improve the energy management of renewable plants with battery storage in capacity firming markets for small, non-interconnected grids [12]. Additionally, the impact of geographically diversifying onshore wind farms has been analyzed as a strategy to reduce required firm capacity and improve system reliability [13].

While previous studies have primarily focused on supply-side solutions for capacity firming, *demand flexibility* has attracted comparatively less attention. In [14], demand flexibility is considered as a physical hedge to limit the price exposure of an aggregator in the wholesale electricity market by using demand curtailment to compensate for the uncertainty and variability of variable renewable energy in the aggregator's portfolio. The authors in [15] considered demand response as one element of the capacity-firming technology suite (along with battery storage, pumped-hydro storage and open-cycle gas generation) to ensure the security of supply of the Spanish electric power system. Additionally, [16] explored how flexible electrification in heating, transport, and industry can support renewable integration and reduce reliance on storage and backup generation, primarily focusing on demand-side adjustments. To our knowledge, our earlier work [17] is the only one that explicitly considered prosumer-owned batteries for capacity firming.

This study considers capacity firming in the context of *future grid scenario analysis* in renewable integration studies that inform policymakers and power system planners about the challenges and opportunities of low-carbon future grids, e.g. Australian Integrated system Plan [2], North American Renewable Integration Study [18], and European ENTSO-E's 10-year network development plan (TYNDP) [19]. Scenario analysis is used to explore and evaluate a range of variables, such as technological developments, policy changes, economic factors, and environmental impacts. Scenario studies typically employ capacity expansion and production cost models to provide the least cost portfolio for the development of a national or continental grid [20]. Capacity expansion models provide a high-level long-term view of the evolving power system by developing a least-cost generation and transmission expansion plan to meet projected electricity demand. Production cost models, on the other hand, simulate power system operations on shorter time scales using detailed load, transmission, and generation fleet data by minimizing production costs [21,22].

[5] Solar self-consumption is the most common optimization strategy in Australia. Because retail tariffs are higher than feed-in tariffs, maximizing solar self-consumption is equivalent to minimizing electricity costs.

1.3. Knowledge gap

The existing literature [9–12,14–16] reveals two critical gaps in the way demand flexibility is modeled for capacity firming. First, current studies address demand flexibility through load reduction or temporal shifting, failing to fully capture the bidirectional potential of prosumer-owned DERs. This limitation restricts the system operator's ability to leverage the dynamic capabilities of distributed resources for effective capacity firming. Existing approaches predominantly focus on unidirectional demand response, overlooking how prosumer-owned DERs can provide bidirectional capacity firming services by absorbing excess renewable generation and exporting power when needed, leading to suboptimal grid balancing, increased renewable curtailment, and a continued reliance on conventional generation sources.

In addition, conventional load flexibility models typically assume a centralized control framework, where controllable loads and VPPs are fully managed by the system operator [23]. However, this approach overlooks the practical reality of private ownership and the operational prerogative of aggregated DERs. The critical challenge is to design optimization and control strategies that prioritize prosumers' private objectives (e.g., maximizing solar self-consumption) while enabling the system operator to access the remaining aggregated capacity for system-level capacity firming. It is essential to ensure that prosumers maintain their expected self-consumption benefits while allowing the system operator to optimize grid operations. Achieving this balance between prosumer prerogative and grid-level coordination remains largely unexplored in the existing literature.

As the main objective of the prosumers is to maximize their PV self-consumption, an appropriate model is required to consider the private objective of the prosumers within the optimization model, minimizing the objective of the system operator. This leads to the creation of a mathematical program with equilibrium constraints (MPEC) [24], where the system operator's optimization problem is constrained by the optimization problems of the prosumers.

The MPEC framework is widely used to model hierarchical decision-making in energy systems, including the strategic bidding behavior of generation companies [25], EV fleet aggregators [26], RES power producers [27], and grid-scale energy storage systems [28]. In these models, the upper-level problem is to find the strategic bidding behavior of the entity owner, while the lower-level problem simulates the market clearing operation. The bilevel structure was also used to model the energy management of a retailer for various distributed resources [29] and the planning design of an EV charging station using RESs [30]. A common approach for integrating the lower-level optimization problem into the upper-level one is to include the lower-level problem optimality Karush-Kuhn–Tucker (KKT) conditions as constraints in the upper-level problem and reformulate it into a single mixed-integer linear program. Therefore, this approach is used in this study.

In contrast to other models that focus on the interaction between an aggregator and prosumers or the aggregator and the wholesale market that use *price coupling* (e.g. [26,31]), the proposed formulation uses *demand coupling*, as in our previous work [32]. Price-coupling approaches define a market structure by establishing a pricing rule to support a particular outcome. In contrast, when the two levels are coupled through the prosumer demand the model becomes agnostic to market pricing mechanisms. It is assumed that an efficient mechanism is in place for prosumer aggregation, with prices determined by that mechanism to support the outcomes computed by the proposed optimization framework.

The demand coupling model allows the system operator to select the most cost-effective solution from the set of multiple prosumer-optimal outcomes. When solar generation significantly exceeds the battery capacity—as is often the case in Australia[6]—prosumers naturally have multiple equally beneficial battery charging and discharging strategies that maximize self-consumption. This flexibility allows the system operator to choose the solution that minimizes generation costs and enhances grid stability without impacting prosumer benefits. Compared to solving the prosumer and system operator problems independently, the bilevel formulation significantly reduces the cost of firming services, as demonstrated in Section 3.4.

To address this, a production cost model suitable for scenario analysis is introduced. The model is conceptually similar to [10], where a unit commitment electricity market model is used to analyze the performance of an open-cycle gas turbine and a large-scale battery system as a physical hedge against volume and price risk in an electricity market. However, the proposed model extends this framework by explicitly incorporating prosumer-owned DERs and comparing their effectiveness with established capacity-firming alternatives.

1.4. Contributions

This paper introduces a novel demand-coupling bilevel optimization framework that enables the system operator to effectively utilize prosumers' unused battery capacity for capacity firming. The framework advances existing knowledge by addressing two key challenges: (1) preserving prosumer prerogative by ensuring that prosumers maximize their self-consumption before offering any remaining capacity to the system operator, and (2) enabling bidirectional demand flexibility to enhance renewable energy integration and reduce reliance on conventional generation.

This paper builds on our earlier conference publication [17] by expanding the scope of discussions and analysis in several significant ways. First, the study moves beyond examining a single wind farm by utilizing a comprehensive production cost model based on a unit commitment problem, which necessitates a different modeling approach, as explained in Section 2.2. Second, the study takes inspiration from the current state of the Australian National Electricity Market (NEM), presenting a practical case study that focuses on prosumer-owned batteries as a source of firm capacity. Using realistic data, the paper provides a reliable assessment of the potential for prosumers to reduce the reliance on utility-scale storage and gas generation as primary sources of firm capacity.

In summary, the main contributions are as follows.

- A novel bilevel capacity firming optimization model is proposed, leveraging unused battery capacity *after* prosumers have optimized solar self-consumption. This model (1) preserves the prosumer prerogative and (2) provides the system operator with the flexibility to choose among multiple optimal solutions of the lower-level problem, ultimately reducing generation costs.
- The study findings demonstrate that utilizing prosumer-owned batteries for capacity firming can significantly reduce the reliance on gas generation and utility-scale batteries while enhancing the economic viability of home batteries.
- The case study reveals a diminishing marginal benefit of capacity-firming services provided by prosumers as their battery size relative to PV capacity increases.

1.5. Organization of the paper

The rest of the paper is organized as follows. Section 2 outlines the problem setup and provides the formulation of the bilevel capacity firming optimization model. Section 3 describes the case studies. Section 5 concludes the paper and provides directions for future work.

[6] In Australia, PV generation can exceed the battery capacity by between at least a factor of 2 in winter and over 8 in summer, assuming a typical 7 kW PV system and a 10 kW h battery.

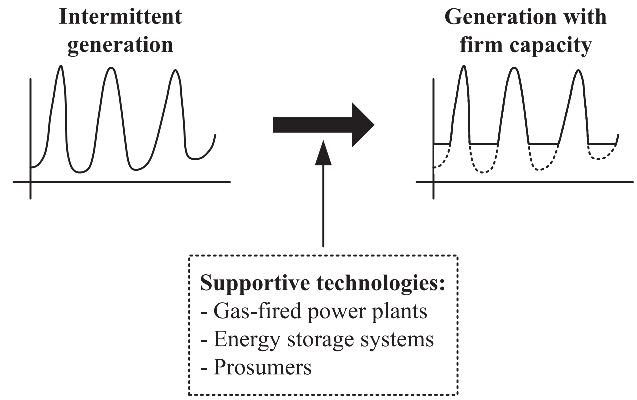

Fig. 1. Conceptual model of capacity firming.

2. Model setup

The model setup aims to provide a structured approach for analyzing the proposed capacity firming framework. This section outlines the key assumptions considered in the study and presents the Capacity Firming Optimization Model.

2.1. Modeling assumptions

The proposed production cost model is based on our previous research [32]. The model, based on a unit commitment problem, has been modified by explicitly including capacity firming, as illustrated in Fig. 1. The following firming technologies are considered:

- Conventional gas-fired power plants,
- Utility-scale batteries,
- Prosumer VPPs that aggregate prosumer-owned batteries.

The model is designed for future grid scenario analysis, aiming to capture the behavior of a hypothetical future grid. The objective of the upper-level market model is to schedule and dispatch power generation at minimum cost to meet the required demand under a set of system-wide constraints, including capacity firming. To preserve computational efficiency, Generation unit clustering is applied [33], along with a DC power flow model to represent the transmission network, while the distribution network is not explicitly modeled, which is a standard approach in high-level system studies [9–15]. Preventing low-voltage distribution network issues (overvoltage and network congestion) can be achieved by introducing flexible export limits (aka operating envelopes), which is an emerging industry practice in Australia [34]. Finally, the formulation of the problem is deterministic. The impact of uncertainty on renewable energy production can be considered using a scenario approach to capture meteorological variability, which is a standard technique in production cost modeling. Alternatively, incorporating uncertainty in bi-level optimization directly can be handled by distributionally robust optimization as in [35], which comes at the cost of the increased computational burden.

The prosumers are aggregated into a single entity and controlled by a VPP operator. Prosumers have smart meters equipped with home energy management systems for scheduling the batteries, and communication infrastructure is assumed to allow two-way communication between the grid, the aggregator and the prosumers, facilitating energy trading between prosumers in the VPP. The proposed model is agnostic with respect to the internal aggregation mechanism. That is, it implicitly assumes that an efficient mechanism for prosumer aggregation is adopted, with prices determined by that unspecified mechanism, which supports the outcomes computed by the proposed optimization framework. However, detailed energy-sharing mechanisms among

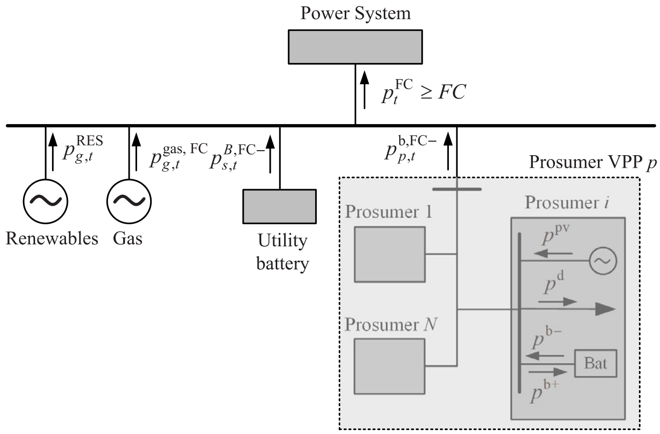

Fig. 2. Conceptual model of using prosumer VPPs $p_{p,t}^{\mathrm{b,FC}-}$ for capacity firming, complementing gas generation $p_{g,t}^{\mathrm{gas,FC}-}$, utility-scale batteries $p_{s,t}^{\mathrm{B,FC}-}$, and renewable energy $p_{g,t}^{\mathrm{RES}}$. The total firm capacity p_t^{FC} must be greater than or equal to the required firm capacity FC, according to (4). Prosumers within the VPP p (shaded area) are not modeled explicitly.

prosumers within VPPs—requiring finer granularity and analyzed in studies such as [36,37]—are beyond the scope of this paper. Instead, this study focuses on the broader, system-wide benefits of VPPs in capacity firming, considering their interaction with the grid rather than the internal financial feasibility of individual prosumers. Full prosumer engagement in offering surplus battery capacity is assumed. However, the social factors [38] and behavioral factors [39] that influence prosumers' willingness to participate in capacity firming beyond financial incentives deserve further attention.

Explicit modeling of long-term battery degradation is not included in the proposed framework to maintain computational efficiency and practical applicability. Instead, degradation is indirectly managed through operational constraints, such as state-of-charge limits and cycling restrictions, ensuring that the battery is not excessively used. This approach aligns with industry practices, where simplified degradation models are preferred for active decision-making [40]. While long-term degradation effects are not explicitly modeled, the proposed framework offers a practical evaluation of the trade-offs between capacity firming participation and battery degradation.

Fig. 2 illustrates the novel concept of using prosumers in capacity firming. Prosumers are aggregated in VPPs where the prosumers inside of the VPP (shaded area) are not modeled explicitly. Prosumer VPPs complement gas generation and utility-scale batteries so that the total firm capacity p_t^{FC} is greater than the required firm capacity FC, as explained in (4) in Section 2.2.2. This scheme assumes that prosumers will use their battery to maximize their self-consumption. Since the battery is not usually completely used up by the prosumer, the remaining capacity can support non-dispatchable generation in meeting the requested capacity firming. This process can be modeled as a bilevel optimization problem. The upper-level optimization problem involves using the remaining battery capacity for capacity firming, while the lower-level problem aims to maximize the prosumer's self-consumption. The upper-level optimization is constrained by the lower-level optimization, and the battery-sharing principle connects the two levels. This principle gives priority to the prosumer as the owner of the battery, which is the key innovation of this work.

2.2. Capacity firming optimization model

The optimization model is divided into an upper-level optimization problem, representing the market operator, which addresses unit commitment and capacity firming, and a lower-level optimization problem that models the behavior of prosumer VPPs.

2.2.1. Upper-level problem (Unit commitment)

The upper-level problem is formulated as a unit commitment (UC) model to represent market operations and optimize power system scheduling. A high-level description of the standard operational constraints is provided here, while the complete mathematical formulations for power reserve, generation, and transmission line limits are detailed in Appendix A for completeness.

$$\begin{aligned}
\text{minimize}\quad & \text{generation cost} \qquad (1)\\
\text{subject to}\quad & \text{power balance constraints,}\\
& \text{power reserve constraints,}\\
& \text{generation constraints,}\\
& \text{transmission line limits,}\\
& \text{capacity firming constraints,}\\
& \text{prosumers VPP KKT conditions.}
\end{aligned}$$

Objective function: The objective of the proposed model is to minimize the total generation cost for all times t:

$$\min_{\Omega} \sum_{t\in\mathcal{T}} \sum_{g\in\mathcal{G}} \left(c_g^{\mathrm{fix}} o_{g,t} + c_g^{\mathrm{su}} u_{g,t} + c_g^{\mathrm{sd}} d_{g,t} + c_g^{\mathrm{var}} p_{g,t} \right), \tag{2}$$

where $\Omega = \{o_{g,t}, u_{g,t}, d_{g,t}, p_{g,t}, p_{s,t}, p_{p,t}, p_{l,t}\}$ is the set of decision variables of the upper-level problem, including the total number of online units at generation plant g, the turning on/off status of power plant g, power generation of power plant g, power of utility-scale battery s, power of prosumer VPP p, and power flow on transmission line l, all in time slot t; c_g^{fix}, c_g^{su}, c_g^{sd}, and c_g^{var} represent fixed, startup, shutdown, and variable costs, respectively.

Power balance: Power generated at node n must be equal to the node power demand, including the transmission losses plus the net power flow on transmission lines connected to the node and charged/discharged power from the prosumer VPP and utility-scale batteries:

$$\begin{aligned}
\sum_{g\in\mathcal{G}_n} p_{g,t} = &- \sum_{g\in\mathcal{G}_n^{\mathrm{gas}}} p_{g,t}^{\mathrm{gas,FC}} + \sum_{c\in\mathcal{C}_n} (1+LF) p_{c,t} \\
&+ \sum_{l\in\mathcal{L}_n} p_{l,t} + \sum_{s\in\mathcal{S}_n} (p_{s,t}^{\mathrm{B}+} - p_{s,t}^{\mathrm{B}-} - p_{s,t}^{\mathrm{B,FC}-}) \\
&+ \sum_{p\in\mathcal{P}_n} (p_{p,t}^{g+} + p_{p,t}^{\mathrm{UL,b}+} - p_{p,t}^{\mathrm{UL,b}-} - p_{p,t}^{\mathrm{b,FC}-}),
\end{aligned} \tag{3}$$

where $\mathcal{G}_n, \mathcal{G}_n^{\mathrm{gas,FC}}, \mathcal{C}_n, \mathcal{L}_n, \mathcal{S}_n, \mathcal{P}_n$ represent the set of generator (including coal, gas, wind and solar, but excluding gas generators used for capacity firming), gas-fired power plants used for capacity firming, consumers (inflexible electricity end users), transmission lines, utility-scale batteries and prosumer VPPs connected to node n, respectively; LF is the loss factor representing system losses modeled as a percentage of system demand $p_{c,t}$; $p_{g,t}^{\mathrm{gas,FC}}$ is the power of gas-fired power plant g used for capacity firming; $p_{s,t}^{\mathrm{B}}$ is the charging/discharging power of utility-scale battery s, $p_{s,t}^{\mathrm{B,FC}}$ is the utility-scale battery power used for capacity firming; $p_{p,t}^{g+}$ is the power consumed by prosumer p, while $p_{p,t}^{\mathrm{UL,b}}$ and $p_{p,t}^{\mathrm{b,FC}}$ are the charging/discharging power and the power used for capacity firming from the remaining VPP p aggregated batteries capacity, all in time slot t. Note that both the utility and the prosumer VPP battery are charged from the grid (using $p_{s,t}^{\mathrm{B},+}$ and $p_{p,t}^{\mathrm{UL,b},+}$, respectively). Hence, $p_{s,t}^{\mathrm{B,FC}+}$ and $p_{p,t}^{\mathrm{b,FC}+}$ are always zero and are omitted in the model.

Power reserve constraints: To take into account uncertainties, active power reserves provided by synchronous generation are always maintained (10% in this paper). The reserves are defined as the difference between the online capacity (the total number of online units at each generation plant) and the current operating point.

Generation constraints: Generation constraints consist of generation production limits, unit on/off constraints, rolling horizon constraints, ramp limits, minimum up and down time, and the number of online units.

Transmission line limits: A DC power flow model is used for computational simplicity. Transmission line limits consist of thermal and stability limits (the voltage angle difference over a transmission line is limited to 30°).

2.2.2. Upper-level problem (Capacity firming)

Using utility-scale batteries and prosumer VPPs for capacity firming requires some additional constraints in the upper-level unit commitment problem.

Firm capacity: As illustrated in Fig. 1, the firm capacity should always be greater than the guaranteed amount FC:

$$p_t^{\mathrm{FC}} = \sum_{g\in\mathcal{G}_n^{\mathrm{RES}}} p_{g,t}^{\mathrm{RES}} + \sum_{g\in\mathcal{G}_n^{\mathrm{gas}}} p_{g,t}^{\mathrm{gas,FC}} - \sum_{s\in S_n} p_{s,t}^{\mathrm{B,FC-}} - \sum_{p\in\mathcal{P}_n} p_{p,t}^{\mathrm{b,FC-}} \geq FC, \tag{4}$$

where $p_{g,t}^{\mathrm{RES}}$ is the generation supplied by RESs, $p_{g,t}^{\mathrm{gas,FC}}$ is the generation of conventional gas-fired power plants, $p_{s,t}^{\mathrm{B,FC-}}$ is power from utility-scale batteries, and $p_{p,t}^{\mathrm{b,FC-}}$ is power supplied by prosumer VPPs.

Utility-scale battery constraints: consist of energy balance (5), capacity, and ramping constraints (6):

$$e_{s,t}^{\mathrm{B}} = e_{s,t-1}^{\mathrm{B}} + \eta^{\mathrm{B+}} p_{s,t}^{\mathrm{B+}} - \frac{p_{p,t}^{\mathrm{B-}}}{\eta^{\mathrm{B-}}} - \frac{p_{p,t}^{\mathrm{B,FC-}}}{\eta^{\mathrm{B-}}}, t \neq 1, \tag{5a}$$

$$e_{s,t}^{\mathrm{B}} = \hat{e}_{s}^{\mathrm{B}} + \eta^{\mathrm{B+}} p_{s,t}^{\mathrm{B+}} - \frac{p_{p,t}^{\mathrm{B-}}}{\eta^{\mathrm{B-}}} - \frac{p_{p,t}^{\mathrm{B,FC-}}}{\eta^{\mathrm{B-}}}, t = 1, \tag{5b}$$

$$\underline{e}_s^{\mathrm{B}} \leq e_{s,t}^{\mathrm{B}} \leq \overline{e}_s^{\mathrm{B}}, \tag{6a}$$

$$0 \leq p_{s,t}^{\mathrm{B+}} \leq r^{\mathrm{B+}} \overline{e}_s^{\mathrm{B}} \Psi_{s,t}^{B+}, \tag{6b}$$

$$0 \leq p_{s,t}^{\mathrm{B-}} + p_{s,t}^{\mathrm{B,FC-}} \leq r^{\mathrm{B-}} \overline{e}_s^{\mathrm{B}} \Psi_{s,t}^{B-}, \tag{6c}$$

$$\Psi_{s,t}^{B+} + \Psi_{s,t}^{B-} \leq 1, \tag{6d}$$

$$\Psi_{s,t}^{B+}, \Psi_{s,t}^{B-} \in \{0,1\}, \tag{6e}$$

where binary variables $\Psi_{s,t}^{\mathrm{B+}}$ and $\Psi_{s,t}^{\mathrm{B-}}$ prevent simultaneous charging and discharging. The ramp rates $r^{\mathrm{B+}}$ and $r^{\mathrm{B-}}$ are given as a fraction of the battery capacity per hour. For example, $0.25\,\mathrm{h}^{-1}$ corresponds to $C/4$ charge/discharge rate, or a *4-h battery* (see the case study in Section 3).

Prosumer VPP storage constraints: A similar model is used to model the battery constraints of the prosumer VPP, except that the storage capacity is split into two components: $e_{p,t}^{\mathrm{UL,b}}$ and $e_{p,t}^{\mathrm{LL,b}}$, representing the stored energy in the prosumer's battery p available in time slot t for exploitation in the upper- and lower-level optimization problem, respectively. The energy balance constraints are

$$e_{p,t}^{\mathrm{UL,b}} = e_{p,t-1}^{\mathrm{UL,b}} + \eta^{\mathrm{b+}} p_{p,t}^{\mathrm{UL,b+}} - \frac{p_{p,t}^{\mathrm{b,FC-}}}{\eta^{\mathrm{b-}}} - \frac{p_{p,t}^{\mathrm{UL,b-}}}{\eta^{\mathrm{b-}}},\ t \neq 1,$$

$$e_{p,t}^{\mathrm{UL,b}} = \hat{e}_{p}^{\mathrm{UL,b}} + \eta^{\mathrm{b+}} p_{p,t}^{\mathrm{UL,b+}} - \frac{p_{p,t}^{\mathrm{b,FC-}}}{\eta^{\mathrm{b-}}} - \frac{p_{p,t}^{\mathrm{UL,b-}}}{\eta^{\mathrm{b-}}},\ t = 1,$$

$$\underline{e}_p^{\mathrm{b}} \leq e_{p,t}^{\mathrm{UL,b}} + e_{p,t}^{\mathrm{LL,b}} \leq \overline{e}_p^{\mathrm{b}}. \tag{7a}$$

The VPP battery charge and discharge used in the upper level is constrained by the use at the lower level:

$$0 \leq p_{p,t}^{\mathrm{UL,b+}} \leq (r^{\mathrm{b+}} \overline{e}_p^{\mathrm{b}} - p_{p,t}^{\mathrm{LL,b+}}) \Psi_{s,t}^{b+}, \tag{8a}$$

$$0 \leq p_{p,t}^{\mathrm{UL,b-}} + p_{p,t}^{\mathrm{b,FC-}} \leq (r^{\mathrm{b-}} \overline{e}_p^{\mathrm{b}} - p_{p,t}^{\mathrm{LL,b-}}) \Psi_{s,t}^{b-}, \tag{8b}$$

$$\Psi_{s,t}^{b+} + \Psi_{s,t}^{b-} \leq 1, \tag{8c}$$

$$\Psi_{s,t}^{b+}, \Psi_{s,t}^{b-} \in \{0,1\}, \tag{8d}$$

similar to (6), $\Psi_{s,t}^{\mathrm{b+}}$, and $\Psi_{s,t}^{\mathrm{b-}}$ are binary variables to prevent simultaneous charging and discharging.

To maintain a harmonized operation of the VPP battery in both upper- and lower-level optimization problems, the following constraints are imposed:

$$0 \leq p_{p,t}^{\mathrm{LL,b+}} \leq \Psi_{s,t}^{b+} M, \tag{9a}$$

$$0 \leq p_{p,t}^{\mathrm{LL,b-}} \leq \Psi_{s,t}^{b-} M, \tag{9b}$$

where M is a sufficiently large constant that is always greater than $p_{p,t}^{\mathrm{LL,b\pm}}$. It is important to note that $e_{p,t}^{\mathrm{LL,b}}$ and $p_{p,t}^{\mathrm{LL,b\pm}}$ are parameters in the upper-level problem, since it is defined in the lower-level problem as explained in Section 2.2.3. Constraint (9) ensures that the system operator's control $\Psi_{s,t}^{\mathrm{b\pm}}$ does not conflict with the actions of the prosumer VPPs, $p_{p,t}^{\mathrm{LL,b\pm}}$.

The bilinear terms $p_{p,t}^{\mathrm{LL,b\pm}} \Psi^{b\pm} s,t$ in (8) are linearized using the big M approach by introducing new variables $\overline{p}p,t^{\mathrm{UL,b\pm}}$:

$$0 \leq p_{p,t}^{\mathrm{UL,b+}} \leq \overline{p}_{p,t}^{\mathrm{UL,b+}}, \tag{10a}$$

$$0 \leq p_{p,t}^{\mathrm{UL,b-}} + p_{p,t}^{\mathrm{b,FC-}} \leq \overline{p}_{p,t}^{\mathrm{UL,b-}}. \tag{10b}$$

To ensure $\overline{p}_{p,t}^{\mathrm{UL,b\pm}} = r^{\mathrm{b\pm}} \overline{e}_p^{\mathrm{b}} - p_{p,t}^{\mathrm{LL,b\pm}}$ only when $\Psi_{s,t}^{\mathrm{b\pm}} = 1$, we introduce the following set of constraints:

$$0 \leq \overline{p}_{p,t}^{\mathrm{UL,b+}} \leq \Psi_{s,t}^{b+} M_1, \tag{11a}$$

$$\overline{p}_{p,t}^{\mathrm{UL,b+}} \leq r^{\mathrm{b+}} \overline{e}_p^{\mathrm{b}} - p_{p,t}^{\mathrm{LL,b+}}, \tag{11b}$$

$$\overline{p}_{p,t}^{\mathrm{UL,b+}} \geq r^{\mathrm{b+}} \overline{e}_p^{\mathrm{b}} - p_{p,t}^{\mathrm{LL,b+}} - (1 - \Psi_{s,t}^{b+}) M_1, \tag{11c}$$

$$0 \leq \overline{p}_{p,t}^{\mathrm{UL,b-}} \leq \Psi_{s,t}^{b-} M_2, \tag{11d}$$

$$\overline{p}_{p,t}^{\mathrm{UL,b-}} \leq r^{\mathrm{b-}} \overline{e}_p^{\mathrm{b}} - p_{p,t}^{\mathrm{LL,b-}}, \tag{11e}$$

$$\overline{p}_{p,t}^{\mathrm{UL,b-}} \geq r^{\mathrm{b-}} \overline{e}_p^{\mathrm{b}} - p_{p,t}^{\mathrm{LL,b-}} - (1 - \Psi_{s,t}^{b-}) M_2. \tag{11f}$$

2.2.3. Lower-level problem (Prosumer operation)

Prosumer VPP objective function: The prosumer objective is to maximize PV self-consumption, which can be modeled as a minimization of residual demand, i.e. the missing energy that must be supplied from the grid, $p_{p,t}^{\mathrm{g+}}$, provided that the feed-in-tariff is always less than the retail tariff (see also Section 1.1). To preserve the linearity of the prosumer VPP battery model (15), a small penalty term is added to the objective function to discourage simultaneous charging and discharging while ensuring that this adjustment does not affect the optimization outcome:

$$\underset{\Omega_p}{\text{minimize}} \sum_{t\in\mathcal{T}} p_{p,t}^{\mathrm{g+}} + c^{\mathrm{pen}} (p_{p,t}^{\mathrm{LL,b+}} + p_{p,t}^{\mathrm{LL,b-}}), \tag{12}$$

where $\Omega_p = \{p_{p,t}^{\mathrm{g+}}, p_{p,t}^{\mathrm{pv}}, p_{p,t}^{\mathrm{curt}}, p_{p,t}^{\mathrm{LL,b+}}, p_{p,t}^{\mathrm{LL,b-}}, e_{p,t}^{\mathrm{b}}\}$ is the set of decision variables of the problem; $p_{p,t}^{\mathrm{LL,b\pm}}$ and $e_{p,t}^{\mathrm{b}}$ represent the charging/discharging power (p), and the energy (e) stored in the prosumer VPP's p battery in time slot t.

Power balance constraints: The demand of the prosumer VPP $p_{p,t}^{\mathrm{d}}$ must be met at every hour:

$$p_{p,t}^{\mathrm{g+}} + p_{p,t}^{\mathrm{pv}} + p_{v,t}^{\mathrm{LL,b-}} = p_{p,t}^{\mathrm{d}} + p_{v,t}^{\mathrm{LL,b+}}, \tag{13}$$

where grid power import $p_{p,t}^{\mathrm{g+}} \geq 0$.

PV power constraints: The following constraints allow the VPP to apply the PV power curtailment $p_{p,t}^{\mathrm{curt}}$ to manage excess generation:

$$p_{p,t}^{\mathrm{pv}} = p_{p,t}^{\mathrm{pv,total}} - p_{p,t}^{\mathrm{curt}}, \tag{14a}$$

$$p_{p,t}^{\mathrm{pv}}, p_{p,t}^{\mathrm{curt}} \geq 0, \tag{14b}$$

Battery storage constraints: Prosumer VPP battery state of charge $e_{p,t}^{\mathrm{LL,b}}$, and $p_{p,t}^{\mathrm{LL,b\pm}}$ are decision variables, not a parameter as in the upper-level problem (7a):

$$e_{p,t}^{\mathrm{LL,b}} = e_{p,t-1}^{\mathrm{LL,b}} + \eta_p^{\mathrm{b+}} p_{p,t}^{\mathrm{LL,b+}} - \frac{1}{\eta_p^{\mathrm{b-}}} p_{p,t}^{\mathrm{LL,b-}}, \qquad t \neq 1, \tag{15a}$$

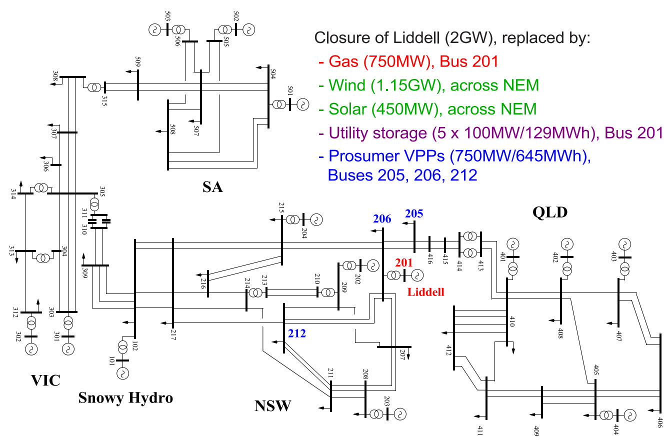

Fig. 3. National Electricity Market (NEM) model based on the 14-generator IEEE test system [42].

$$e_{p,t}^{\mathrm{LL,b}} = \hat{e}_p^{\mathrm{LL,b}} + \eta_p^{\mathrm{b+}} p_{p,t}^{\mathrm{LL,b+}} - \frac{1}{\eta_p^{\mathrm{b-}}} p_{p,t}^{\mathrm{LL,b-}}, \qquad t = 1, \tag{15b}$$

$$\underline{e}_p^{\mathrm{b}} \le e_{p,t}^{\mathrm{LL,b}} \le \overline{e}_p^{\mathrm{b}}, \tag{15c}$$

$$0 \le p_{p,t}^{\mathrm{LL,b+}} \le r^{\mathrm{b+}} \overline{e}_p^{\mathrm{b}}, \tag{15d}$$

$$0 \le p_{p,t}^{\mathrm{LL,b-}} \le r^{\mathrm{b-}} \overline{e}_p^{\mathrm{b}}. \tag{15e}$$

The battery model (15) ensures that charging and discharging do not occur simultaneously. This is enforced by requiring both the charging and the discharging power to be non-negative, (15d) and (15e), and by including the penalty term $c^{\mathrm{pen}}(p_{p,t}^{\mathrm{LL,b+}} + p_{p,t}^{\mathrm{LL,b-}})$ in the cost function (12). If the optimization problem has a feasible solution with both $p_{p,t}^{\mathrm{LL,b-}} > 0$ and $p_{p,t}^{\mathrm{LL,b+}} > 0$, a lower-cost solution can be achieved by setting one of these values to zero while keeping the other positive [41].

To solve the bilevel optimization problem, the lower-level problem (prosumer VPPs) is replaced by its KKT optimality conditions, which are sufficient for optimality, and incorporated as constraints into the upper-level problem (unit commitment), as shown in (1). The complementary slackness conditions in the KKT formulation introduce bilinear terms, which are linearized using the big M method, transforming the problem into a single mixed-integer linear program. This reformulation enables the efficient solution of the bilevel optimization problem using standard MILP solvers. Further details on the derivation and implementation of the KKT conditions are provided in Appendix B.

3. Case study

As a case study, we use the 14-generator IEEE test system shown in Fig. 3. The test system, initially proposed by [42] for small-signal analysis, is loosely based on the Australian National Electricity Market (NEM), the interconnection that spans the eastern Australian coast. The network is stringy, with large transmission distances and loads concentrated in a few load centers. It consists of 59 buses, 28 loads, and 14 generators. The test system consists of four areas representing the states of Queensland (QLD), New South Wales (NSW), Victoria (VIC), and South Australia (SA). In the business as usual (BAU) scenario, the conventional generation portfolio consists of 23.11 GW of black coal, 15.58 GW of brown coal, 5.22 GW of gas, and 2.33 GW of hydro generation.

The case study is motivated by the retirement of the Liddell coal-fired power station in April 2023. AGL, the owner of Liddell, proposed to replace it with a combination of 750 MW of gas, 1.6 GW of wind and solar, 250 MW of utility-scale battery storage and 100 MW of demand response [43]. Wind, solar and load traces are from the Australian Energy Market Operator's (AEMO) National Transmission Network Developed Plan (NTNDP) [44], and the fuel costs are from AEMO's Integrated System Plan [2].

Note that the objective of this case study is not to model the current generation mix in the NEM, but rather to demonstrate how conventional coal-fired generation can be replaced with a mix of gas, utility-scale battery storage, and demand response to guarantee a specified level of firm capacity. Three cases are considered:

- **Case 1 (C1):** BAU with Liddell closed down (2 GW), and replaced with 1.15 GW wind and 450 MW solar spread across the system, and five gas units with a total capacity of 750 MW connected at the location of Liddell (Bus 201).
- **Case 2 (C2):** This is the same as case C1 with an additional installed utility-scale battery connected at Bus 201. The storage capacity varies between one and five times the capacity of the Hornsdale Power Reserve (HPR) 'big battery'.[7] For example, scenario C2-S3 has three HPR worth of capacity (3×129 MWh = 387 MWh). A $C/4$ discharge rate (129 MWh/4 = 32.25 MW) is considered; this contrasts to the faster rate (129 MWh/100 MW) of the Hornsdale battery, which was designed primarily to provide fast frequency control.
- **Case 3 (C3):** This is the same as case C1 with additionally connected prosumer VPPs connected to Buses 205, 206, and 212, with a total rooftop PV capacity of 750 MW and the total battery capacity varying from one to five HPR. For example, scenario C3-S3 has 750 MW worth of PV capacity and three HPR worth of battery storage capacity (3×129 MWh). The same discharge rates $C/4$ as in case C2 are considered. Furthermore, the impact of the discharge rate ($C/4$, $C/2$, $C/1$) is analyzed in the sensitivity analysis in Section 3.6.

The purpose of the sensitivity analysis (scenarios C2-S1 to C2-S5 and C3-S1 to C3-S5) is to analyze the extent to which prosumer-owned batteries can replace utility-scale batteries with the same capacity. In the battery-cycling analysis in Section 3.3, an additional scenario, C3-S10, is included, where the battery capacity is double that of scenario C3-S5.

3.1. Commitment of gas units

This section examines the use of utility-scale batteries and prosumer VPPs for capacity firming to reduce the requirement for gas generation. Fig. 4 compares the results for cases C2 and C3 (blue histograms) with the results for case C1 (red stars), showing the commitment of gas units, from one to five, of the 750 MW gas power plant used for capacity firming. The commitment is measured as the total number of operating hours in the simulated year for each individual unit. Observe that the commitment of gas units is reduced with the increased firm capacity support provided by the utility-scale battery in case C2 and the prosumer VPPs in case C3. Utility-scale batteries demonstrate higher effectiveness due to their dedicated availability and centralized control, enabling more efficient dispatch for capacity firming. They can be strategically located and optimized for maximum grid support, making them a more reliable alternative. In contrast, prosumer VPPs leverage existing DERs, offering a cost-effective and decentralized solution without additional infrastructure investment. Despite their lower availability—primarily due to their role in maximizing self-consumption—they enhance grid resilience and improve overall system flexibility. However, their participation in capacity firming depends on prosumer engagement and appropriate market incentives to ensure adequate availability.

[7] Hornsdale Power Reserve was the largest lithium-ion battery in the world at 100 MW/129 MWh when installed in 2017. It is co-located with the Hornsdale Wind Farm in South Australia.

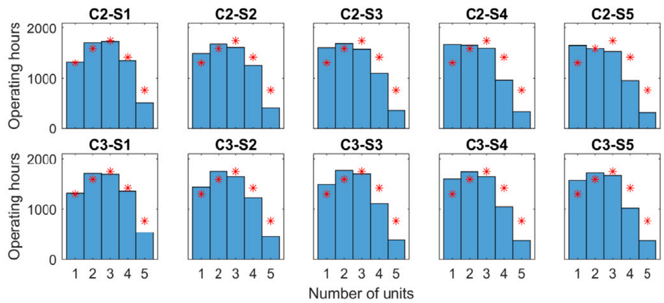

Fig. 4. Commitment of gas units for capacity firming. For comparison purposes, the red stars show the results for case C1 where only gas is used for capacity firming. In cases C2 (top row), and C3 (bottom row), utility-scale batteries and prosumer VPPs, respectively, are used in addition to gas.

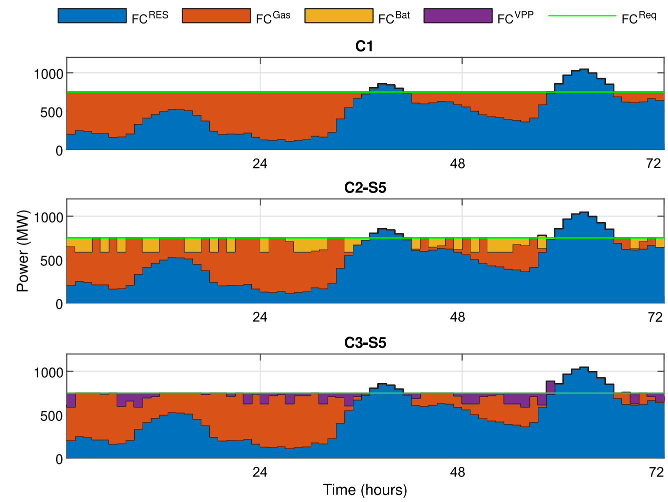

Fig. 5. Firm capacity (FC) traces for different technologies: gas only (C1), gas with utility-scale batteries (C2), and gas with prosumer VPPs (C3) for a typical 72-h period. Only scenarios S5 with storage capacity of 5 ×129 MWh = 645 MWh are shown. Battery discharge rate in C2 and C3 is $C/4$ (645 MWh/4 = 161.25 MW).

3.2. Energy flow analysis

This section examines energy flows both at the system level and at the prosumer level to understand the contributions of various firming resources.

3.2.1. System-level energy flows

The firm capacity traces for three randomly selected days are presented in Fig. 5. Scenarios C2-S5 and C3-S5 are compared with reference case C1, demonstrating the dynamic behavior of utility-scale batteries and prosumer VPPs in capacity firming and the reduction of gas generation in firming renewable generation capacity. In periods of low renewable generation, utility-scale batteries and prosumer VPPs provide some of the firm capacity, reducing the need for gas generation. As expected, utility-scale batteries are more effective as they are only used for capacity-firming purposes; prosumer batteries, on the other hand, are also used for maximizing prosumer PV self-consumption as illustrated in Section 3.2.2. However, despite their contributions, gas units continue to operate extensively, highlighting their critical role in ensuring grid reliability. While utility-scale batteries offer superior performance in terms of efficiency and centralized control, their participation in capacity firming remains limited by scalability challenges, requiring significant investment and infrastructure for widespread deployment. The increasing integration of prosumer VPPs presents an opportunity to address some of the scalability limitations of utility-scale batteries. By leveraging distributed residential storage, prosumer VPPs can contribute to capacity firming on a broader scale, potentially reducing reliance on gas generation. However, their effectiveness is constrained by intermittent availability due to charging cycles and self-consumption priorities. While greater penetration of prosumer batteries could significantly alleviate dependency on gas, they are unlikely to fully replace it. Instead, an optimized combination of gas generation, utility-scale batteries, and prosumer VPPs can offer a more balanced and resilient approach to firm capacity, ensuring system reliability during periods of low renewable output.

3.2.2. Prosumer-level energy flows

Fig. 6 illustrates the energy flows of prosumer VPP at Bus 212 in a typical week for scenario C3-S5. The figure shows prosumer power flows, including electricity demand, PV generation and grid power flow with and without capacity firming (top); battery power flows and state-of-charge for PV self-consumption only (middle); and battery power flows and state-of-charge for PV self-consumption and capacity firming (bottom). The first figure illustrates how prosumers first meet their power demand using PV generation, with any remaining power being imported from the grid. When PV exceeds the demand, the battery first stores extra power and uses it later to meet the demand when PV generation drops. Observe that when prosumers participate in capacity firming, they occasionally send power back to the grid per (4). The battery behavior, when used for maximization of PV-self-consumption only, is illustrated in the middle figure. Finally, the bottom figure illustrates the complete battery behavior, showing the battery state-of-charge for PV self-consumption maximization and capacity firming separately. Observe how part of the battery capacity unused in self-consumption maximization is used for capacity firming; this increases battery cycling analyzed next.

3.3. Battery cycling analysis

The simple rainflow-counting algorithm proposed in [45] is applied to analyze the increased battery cycling due to the participation of prosumers in capacity firming. The algorithm has been used previously in similar applications, e.g. [46,47]. The results are summarized in Table 1, showing the number of annual battery cycles for the three VPPs for all scenarios. The results are split to the number of cycles for PV self-consumption maximization (SC), capacity firming (CF) and the total number of cycles (note that the total number of cycles might not be equal to SC+CF). For illustration purposes, an additional scenario, C3-S10, is included, where the battery capacity is double that of scenario C3-S5.

Several trends are notable. First, the annual number of cycles when the battery is used for self-consumption only is close to the number of days in the year; this reflects the fact that the PV capacity is large enough to fully charge the battery every day. However, when the battery capacity is significantly increased in scenario C3-S10, the battery becomes too large, so it is only charged to less than half of the capacity on average. Second, when the battery is also used for capacity firming, the number of cycles more than doubles because the unused battery capacity is made available for capacity firming, as illustrated in Fig. 6.

The increased cycling might be prohibitive for the most common Lithium Nickel Manganese Cobalt Oxide chemistry (e.g. Tesla Powerwall 2) that is warranted for 3000 cycles (about ten years with one daily cycle). However, Lithium Iron Phosphate (LFP) batteries (e.g. Tesla Powerwall 3) have much better cycling performance. According to [48], they can sustain up to 10,000 cycles at $C/4$ (the base discharge rate assumed in this paper) and 75% depth of discharge. Lithium Titanate batteries have an even better cycling performance. They can be fully charged and discharged for more than 30,000 cycles, but they are more expensive [49].

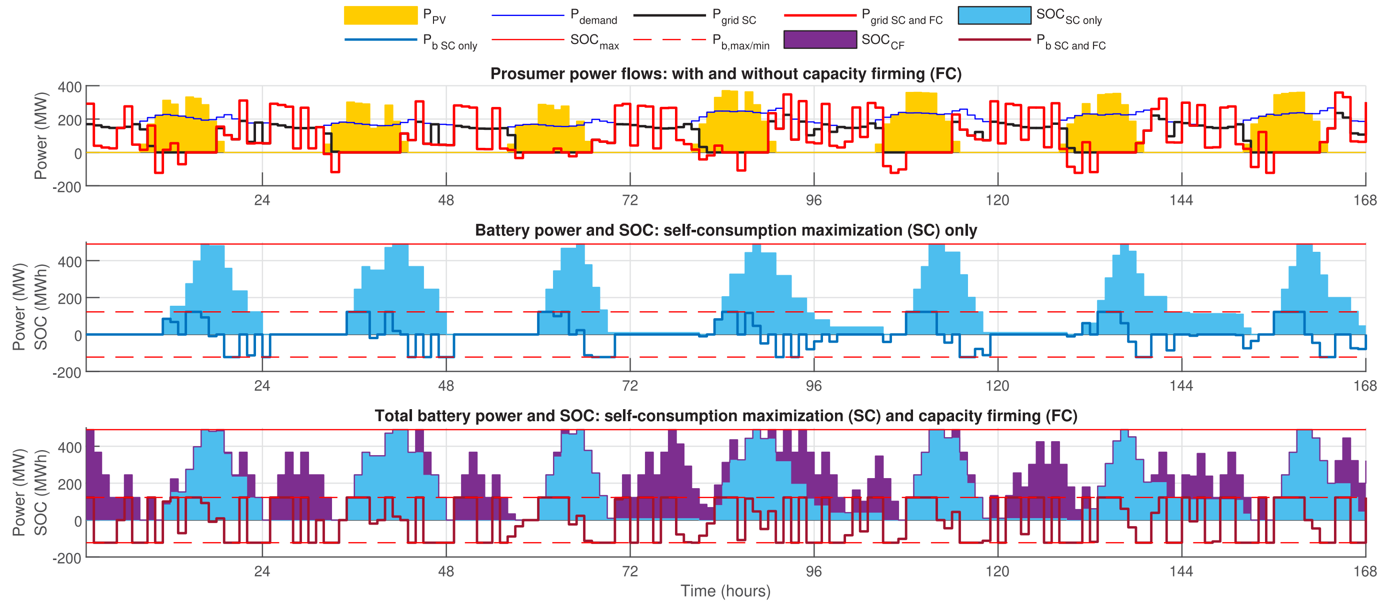

Fig. 6. Prosumer VPP at Bus 212 for scenario C3-S5 for a typical week: prosumer power flows, including electricity demand (P_{demand}), PV generation (P_{PV}) and grid power flow with ($P_{\text{grid SC and FC}}$) and without ($P_{\text{grid SC}}$) capacity firming (top); battery power flows and state-of-charge for, respectively, PV self-consumption only ($P_{\text{b SC only}}$, $SOC_{\text{SC only}}$) (middle) and PV self-consumption and capacity firming ($P_{\text{b SC and FC}}$, SOC_{CF}) (bottom).

Table 1
Battery cycling comparison.

Scenario	VPP Bus 205			VPP Bus 206			VPP Bus 212		
	SC	CF	Tot	SC	CF	Tot	SC	CF	Tot
C3-S1	298	390	534	358	384	537	296	393	541
C3-S2	269	388	536	354	380	538	266	392	534
C3-S3	242	385	535	350	382	542	239	391	515
C3-S4	220	386	527	345	385	539	217	393	499
C3-S5	201	386	520	339	382	534	199	386	487
C3-S10	129	343	485	296	376	508	126	336	464

3.4. Economic analysis

To fully evaluate the benefits of capacity firming on power system operations, it is important to consider its economic advantages and its impact on overall operational costs. Table 2 shows the total annual system costs for the three cases, including all scenarios. These costs cover the whole system and the annual cost of the gas power plant at Bus 201, factoring in fixed, cycling (i.e., start-up and shut-down) and variable operating costs. Case C1 has the highest costs among the three, with a total system cost of 6993 million AU$ and a capacity firming cost of 318 million AU$, as firming is fully provided by gas generation. The addition of battery storage for capacity firming in Cases C2 and C3 leads to higher utilization of renewable generation and consequently to lower operating costs. Focusing specifically on the reduction of the operating costs of the gas power plant used for capacity firming, the costs drop by 22.3% in Scenario C2-S5. By comparison, the proposed prosumer VPP model reduces the operating cost of the gas power plant by 14.5% in scenario C3-S5.

To assess the value of the capacity firming service provided by prosumers, we consider a home battery size of 10 kWh.[8] The annual value of capacity firming per battery is determined by dividing the total reduction in firming costs provided by the gas power plant at Bus 201 (tenth column in Table 2) by the number of batteries in a given scenario (with 12,900 home batteries equivalent to one 129 MWh utility-scale battery). The results, illustrated in Fig. 7, show that for the base case ($C/4$), the value ranges from AU$946/year (C3-S1) to AU$735/year (C3-S5).

This analysis provides a glimpse into the additional value streams available to prosumers, potentially accelerating the adoption of home batteries and reducing carbon emissions by enabling greater penetration of variable renewables. Furthermore, these findings suggest that the proposed model could be a viable solution to address the cost and site challenges associated with large-scale batteries in the long term. However, the results also reveal diminishing marginal benefits as battery adoption increases, emphasizing the need for adaptive policies and market mechanisms that align incentives with evolving grid conditions.

3.5. The value of the bilevel formulation

The last column in Table 2 shows the cost reduction when the lower problem is solved separately (without using the bilevel formulation). The analysis is only applicable to Case 3. Compared to the case where the two optimization problems are solved independently, the system cost reduction increases by between 45% (C3-S1) and as much as 82% (C3-S2). This is because the lower-level problem has several optimal solutions (the same objective values but different values of the decision variables), which gives the market operator the flexibility to choose the one that maximizes the upper-level objective.

3.6. Discharge rate sensitivity analysis

Finally, a sensitivity analysis is conducted, considering battery discharge rates of $C/4$, $C/2$, and $C/1$; the results are shown in Fig. 7. Observe that with increasing discharge rate, the capacity firming value increases significantly, up to AU$3179 for $C/1$ in scenario C3-S1.

This is due to the significantly higher discharge rate (645 MW for $C/1$ compared to 161 MW for $C/4$, combined for the three VPPs). The downside is significantly increased cycling – from 485 annual cycles for $C/4$ in Scenario C3-S5 to 1912 cycles for $C/1$. This is illustrated in Fig. 8, using the same random three-day period as in Fig. 5. The figure

[8] This corresponds to a 14 kWh battery with 70% of usable capacity (state of charge between 15% and 85%), such as the Tesla Powerwall. At a typical residential battery cost of AU$1000/kWh, a 14 kWh system amounts to approximately AU$14,000. Although the model assumes Li-ion chemistry due to its widespread adoption, it can be adapted to other technologies by adjusting parameters such as depth of discharge, charge/discharge rates, and efficiency.

Table 2
Cost comparison for all scenarios for discharge rate of $C/4$. All values are in million AU$.

Scenario	System cost				Gas @Bus 201 cost			Cost reduction		Cost reduction w/o bilevel	
	Fixed	Cycling	Variable	Total	Fixed	Variable	Total	System	Gas @Bus 201	System	Gas @Bus 201
C1	2075.7	113.8	4803.9	6993.4	42.4	276.2	318.6	–	–	–	–
C2-S1	2074.0	114.3	4792.3	6980.6	39.4	260.9	300.3	12.8	18.4	–	–
C2-S2	2073.2	113.6	4780.4	6967.3	36.8	246.6	283.4	26.1	35.2	–	–
C2-S3	2071.8	115.0	4769.6	6956.4	35.0	234.0	269.0	37.0	49.6	–	–
C2-S4	2073.1	113.2	4761.4	6947.7	33.7	223.8	257.5	45.7	61.2	–	–
C2-S5	2070.7	112.5	4752.3	6935.5	32.7	212.6	245.3	57.9	73.3	–	–
C3-S1	2068.8	116.3	4795.4	6980.5	39.5	266.9	306.4	12.9	12.2	8.4	7.7
C3-S2	2065.0	116.9	4786.6	6968.6	37.5	258.2	295.8	24.8	22.9	12.6	13
C3-S3	2062.4	115.5	4778.6	6956.5	36.2	250.6	286.8	36.9	31.8	21.5	17.5
C3-S4	2060.2	117.3	4771.4	6948.9	35.3	243.3	278.6	44.5	40.1	24.7	23.3
C3-S5	2059.4	115.5	4764.4	6939.3	35.1	236.2	271.2	54.1	47.4	31.3	26.1
C3-S10	2052.3	112.2	4729.3	6893.9	31.7	200.5	232.3	99.5	86.4	56.6	48.3

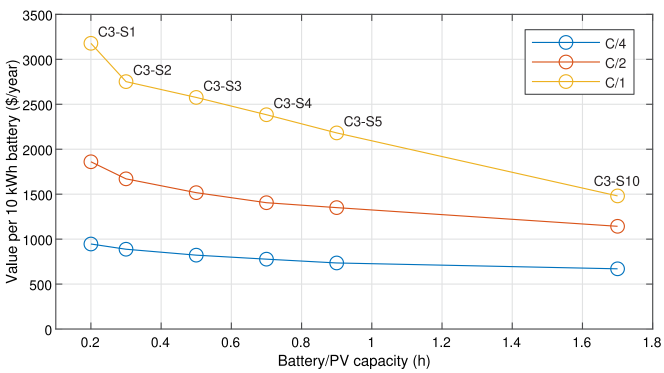

Fig. 7. Annual value of capacity firming services for a 10 kWh home battery. The x-axis shows hours of storage given as the ratio between battery (in kWh) and PV capacity (in kW) in the VPP. The results are shown for three different battery discharge rates: $C/1$, $C/2$ and $C/4$.

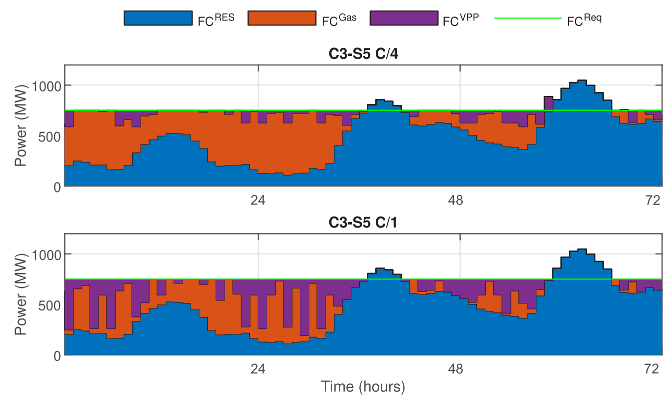

Fig. 8. Firm capacity traces for scenario C3-S5; $C/4$ discharge rate (top), $C/1$ discharge rate (bottom). The base case (C3-S5 $C/4$) is the same as the bottom plot in Fig. 5.

compares Scenario C3-S5 for discharge rates of $C/4$ (base case analyzed in Section 3.2.1) and $C/1$. The increased cycling behavior is, to some extent, an artifact of modeling the VPP battery as a single large battery. The increased cycling is the result of battery discharging to prevent turning on an additional gas turbine. Due to the gas start-up cost, it is more efficient to overcharge the battery in the previous time step and discharge it in the next to avoid turning on an additional gas turbine. The behavior becomes noticeable when the discharge rate increases over $C/3$. In practice, the aggregate VPP battery consists of many small batteries, so this increased cycling would not occur. Therefore, a more granular battery model is needed to obtain a reliable estimate of the cycling behavior for higher discharge rates. However, increasing the discharge rate could potentially result in excessive grid exports. For example, the $C/1$ discharge rate for a 10 kWh home battery means the 10 kW discharge power, which exceeds the 5 kW limit for single-phase connections used in Australia.

3.7. Computational performance

All simulations were conducted using a rolling-horizon approach with hourly resolution. Each optimization encompasses a 48-h look-ahead window with a 24-h overlap over a one-year period, resulting in a total of 138,336 decision variables (22,656 binary, 4896 integer, and 110,784 continuous) and 234,288 constraints per run. The model was implemented in `AMPL` and solved using `Gurobi 11.0` with a 0.5% optimality gap tolerance. All experiments were conducted on a 2.80 GHz quad-core machine with 16 GB of RAM.

Fig. 9 (top) shows the solution times per run in all scenarios, demonstrating that scenarios with prosumer VPPs used for capacity firming are computationally more expensive but still computationally tractable. To further examine scalability, a VPP in Bus 205 (130 MW aggregated rooftop PV, 115 MWh battery) was replicated up to 27 times and analyzed for two simulation horizons, 48-h (Fig. 9 bottom left) and 24-h (Fig. 9 bottom right). Observe that in both cases the computation time grows exponentially as more VPPs are connected in the systems. At the same time, the simulation time grows with increasing horizon length. Nevertheless, the simulation time remains reasonable in both cases, indicating the practicality of the proposed approach. Even in relatively large problem instances, the model converges within computational times that are suitable for both day-ahead market participation and rolling-horizon operational planning.

4. Discussion and open research questions

The case study has demonstrated the value of home batteries in providing capacity-firming services, which can be used in the design of the policy and regulatory framework to incentivize the adoption of home batteries. However, many areas require further research, as discussed below.

4.1. Prosumers participation and policy recommendations

The study does not explicitly model participation rates; however, the scenario analysis accounts for their effects by adjusting the total aggregated battery capacity. For example, in Scenario C3-S1, where 20% of the total potential capacity is used, a low percentage of the participation of the consumer is assumed (20% of eligible consumers adopt batteries). In contrast, Scenario C3-S5 represents full adoption, with 100% of the capacity in use. The results highlight a nonlinear trend: increasing capacity from S1 (20%) to S2 (40%) reduces capacity firming costs by 3.46%, but a further increase from S4 to S5 produces

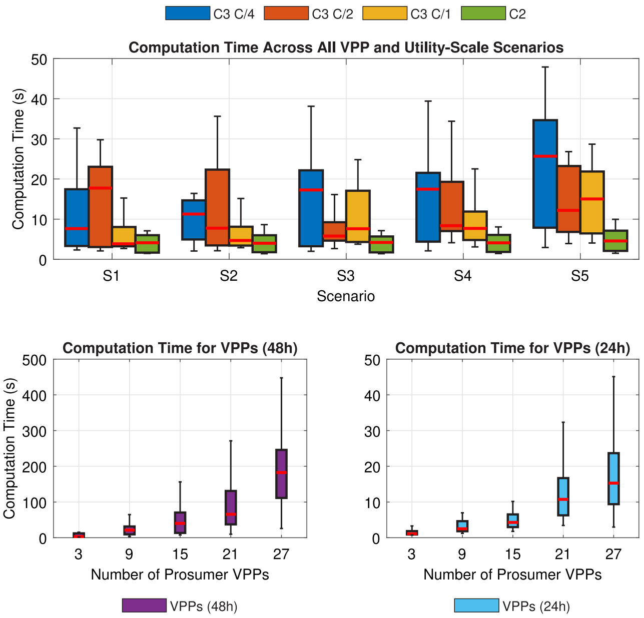

Fig. 9. (Top) Computational performance across large-scale battery C2 (S1–S5) and prosumer VPPs C3 (S1–S5) for charge rates of C/4, C/2, and C/1. (Bottom) Scalability analysis of the proposed model with an increasing number of prosumer VPPs under a rolling horizon with 48-h and 24-h windows.

a smaller improvement, with only a total reduction of 2.66%. This suggests that the greatest benefits occur during the early stages of adoption (20%–40%), while higher adoption levels lead to diminishing returns.

To translate these insights into actionable policy, one avenue involves tiered financial incentives. Early adoption tax credits can stimulate home battery adoption in regions where participation rates remain below 40%, offering, for example, a 30% tax credit that gradually reaches 10% once adoption surpasses 70%. This approach mirrors the Small-scale Renewable Energy Scheme (SRES) in Australia[9] and aligns with the threshold observed between C3-S1 and C3-S2. Meanwhile, degradation compensation in the form of annual payments (e.g., AU$ 50–100/kWh/year) can offset the accelerated battery wear that comes from capacity firming at varying discharge rates ($C/4$ to $C/1$), as highlighted in Section 3.6.

Beyond financial incentives, demand response and VPP integration offer a pathway to improve market participation. Standardized VPP contracts with transparent compensation structures (e.g., AU$ 946/year for $C/4$ discharge), liability provisions, and minimum commitment periods (3–5 years) can lower administrative barriers for prosumers and aggregators alike. Paired with dynamic export limits, such as operating envelopes that allow for an increased export threshold (5 kW to 10 kW) during peak demand—these measures help prevent localized grid congestion while maximizing distributed contributions.

A final consideration involves behavioral and regulatory frameworks. Granting prosumers automated opt-out clauses allows them to prioritize self-consumption during critical periods, such as heatwaves, without facing penalties, thus balancing autonomy with grid support. Furthermore, regulating annual cycling caps (for example, 250 cycles/year) ensures alignment with LFP battery warranties (Section 3.3), safeguarding the long-term viability of storage owned by consumers. These measures collectively speak to the diminishing marginal benefits observed in the case study (Fig. 7) and address the saturation effects of high participation rates. By incentivizing early adoption and promoting decentralized storage, policymakers can replicate the cost reductions seen in C3-S1 to C3-S5 while strengthening the reliability of the grid through distributed resilience. Future work should explore dynamic incentive structures that adjust to evolving participation levels and changing grid conditions.

[9] cer.gov.au/schemes/renewable-energy-target/small-scale-renewable-energy-scheme.

4.2. Financial viability of home batteries

Economic viability is an important consideration when discussing regulatory and policy incentives. Although the study provides an estimate of additional value streams available to prosumers offering capacity-firming services, a detailed analysis of the financial viability of home batteries is out of scope due to the approximations required in production cost modeling. As discussed in Section 2.1, the study focuses on the transmission network, implicitly modeling distribution networks as a copper plate. Furthermore, the demand coupling assumption abstracts away distribution tariffs that are crucial in the cost–benefit analysis of home batteries.

Despite these modeling limitations, the study provides a reasonable estimate of how capacity-firming services impact the economic viability of home batteries. For a typical 14 kWh residential battery priced at approximately AU$14,000, the results in Section 3 suggest a simple payback period of 14 to 20 years for Cases C3-S1 and C3-S5, respectively, when considering capacity firming alone. However, the primary financial benefit of home batteries comes from PV self-consumption. Given a 10-year warranty period, each battery would need between AU$400 and AU$700 in additional annual savings from PV self-consumption to break even. A recent Australian study [50] indicates that achieving these savings is feasible, even without government subsidies. That said, a more detailed analysis—incorporating distribution network modeling and varying residential electricity tariffs—is necessary for actionable policy and regulatory recommendations.

4.3. Long-term sustainability of home batteries

The economic viability of prosumer batteries for capacity firming must be weighed against their environmental footprint. Although lifecycle emissions and material scarcity fall outside the scope of this study, they represent critical barriers to scaling. The production of lithium-ion batteries contributes 40–70% of lifecycle emissions due to the energy-intensive extraction of lithium, cobalt, and nickel [51]. For example, LFP batteries, though cobalt-free, lead to higher lithium demand, potentially straining global supply chains projected to face shortages in the near future [52].

Recycling innovations—such as low-temperature hydrometallurgical processes, which can recover over 90% of metals [53], or direct recycling methods that significantly reduce energy usage—have the potential to substantially reduce lithium demand in the coming decades. Some scenario-based studies suggest that the widespread adoption of advanced recycling could reduce the need for newly mined lithium by as much as 90% by 2060 [54]. However, the current recycling infrastructure remains underdeveloped, and high-emission pyrometallurgical methods remain dominant despite their notable higher greenhouse gas output [55]. Policy frameworks such as EU recycling content mandates (for example, 12% cobalt, 4% lithium by 2030) and US tax incentives for domestic recycling could accelerate progress [56]. Although this study does not model these sustainability factors, their resolution is critical to ensure that home batteries are aligned with global decarbonization goals.

Exploring alternative chemistries, such as sodium-ion or lithium-sulfur batteries, may alleviate material constraints [57], while second-life applications (e.g. repurposing retired batteries for grid storage) can extend usage before recycling [58]. Circular economy principles, including standardized designs for easier disassembly and blockchain-based material tracking, could further reduce lifecycle impacts [59].

For example, automated disassembly of modular battery packs has shown promise in significantly reducing recycling costs [60]. A holistic approach integrating lifecycle-aware policies, recycling innovation, and ethical sourcing is essential to ensure home battery deployment advances decarbonization without compromising resource equity or environmental integrity.

4.4. System reliability and grid resilience

Decentralized capacity firming can strengthen grid reliability but also introduces trade-offs. Battery ownership by prosumer reduces the dependence on centralized infrastructure and, in high penetration scenarios, can support local feeders such as islands microgrids during outages [61]. Their distributed nature mitigates single points of failure, improving resilience to extreme weather events. However, prosumer priorities, particularly self-consumption, limit surplus battery capacity when solar output is low (e.g., cloudy days or nighttime), creating uncertainty in firm capacity. By contrast, gas peaker plants offer dispatchable power and grid-stabilizing inertia during renewable shortfalls, but their centralized configuration is vulnerable to supply disruptions (e.g., pipeline failures) and site-specific risks like flooding. Meanwhile, utility-scale batteries avoid the behavioral uncertainties of prosumer systems, yet still face resilience limitations (e.g., transformer failures, cyberattacks), underscoring the inherent trade-offs among various capacity-firming approaches.

Moving forward, addressing behavioral uncertainties in prosumer adoption and state-of-charge management is crucial for enhancing decentralized storage reliability. Research might focus on quantifying reliability metrics for prosumer-centric grids and developing resilience-aware bidding strategies for VPPs, leveraging probabilistic models. Hybrid systems that combine prosumer-owned VPPs with utility-scale storage could balance flexibility and predictability.

As prosumers independently finance their battery systems for self-consumption rather than as grid investments, their contribution to the grid is best quantified through the reduction in total capacity firming costs. Moreover, to incorporate long-term planning factors—such as the investment costs of gas generation and large-scale batteries alongside operational expenses—a hybrid framework is necessary. This framework should integrate production cost simulations with capacity expansion optimization, providing a more comprehensive economic assessment of prosumer participation. By doing so, it not only captures the reduction in capacity firming costs from an operational standpoint but also accounts for the avoided investments in large-scale batteries and gas generation, which warrant further consideration. While this study focuses on operational cost savings, future research should evaluate the long-term investment implications of these technologies within a capacity expansion framework.

5. Conclusion

This paper is motivated by two important factors in Australia and globally—the increasing use of variable renewable energy and the upcoming closure of coal power plants. However, there is an opportunity to use the growing number of prosumer-owned batteries to help ensure a stable energy supply. To realize this opportunity, this paper has proposed a bilevel capacity firming optimization model that allows prosumers to use their batteries for their private objectives first and offer the remaining capacity to the system operator for capacity firming. It adopts a generic unit commitment approach with demand coupling, ensuring adaptability to diverse market designs and future grid scenarios.

The case study demonstrates the value of prosumer batteries by showing that they are a feasible and effective alternative to conventional gas generation and utility-scale batteries. This indicates a possible direction of the energy policy supporting the energy transition—instead of supporting utility-scale solutions, policymakers should incentivize the adoption of behind-the-meter resources. The results demonstrate the potential economic benefits of distributed storage. However, while the study results can inform policies to incentivize home battery uptake, they should be supported by a detailed cost–benefit analysis.

Additionally, future work should explore the integration of electric vehicles with vehicle-to-grid capabilities, as their larger storage capacities offer substantial firming potential and can complement home batteries in tackling scalability challenges, further reinforcing the role of distributed energy resources in the energy transition.

CRediT authorship contribution statement

Mohsen Aldaadi: Writing – original draft, Visualization, Validation, Methodology, Investigation, Formal analysis, Data curation, Conceptualization. **Miloš Pantoš:** Writing – original draft, Visualization, Validation, Methodology, Investigation, Formal analysis, Data curation, Conceptualization. **Shariq Riaz:** Writing – review & editing, Visualization, Methodology, Conceptualization. **Archie C. Chapman:** Writing – review & editing, Methodology, Conceptualization. **Gregor Verbič:** Writing – review & editing, Supervision, Project administration, Methodology, Conceptualization.

Declaration of competing interest

The authors declare that they have no known competing financial interests or personal relationships that could have appeared to influence the work reported in this paper.

Appendix A. Upper-level operational constraints

Power reserve constraints:

$$\sum_{g\in\{\mathcal{G}^{\text{syn}}\cap\mathcal{G}^{\text{r}}\}} (\overline{p}_g o_{g,t} - p_{g,t}) \geq \sum_{n\in\mathcal{N}_r} p^{\text{rsv}}_{n,t}, \tag{A.1}$$

where sets $\mathcal{G}^{\text{r}}$ and $\mathcal{N}_r$ denote generators and buses within region r. This formulation ensures that each region maintains adequate reserves $p^{\text{rsv}}_{n,t}$ to accommodate real-time uncertainties and maintain system reliability.

Generation limits: Dispatch levels of a synchronous generator g are limited by the respective stable operating limits:

$$o_{g,t}\underline{p}_g \leq p_{g,t} \leq o_{g,t}\overline{p}_g, \quad g\in\mathcal{G}^{\text{syn}}. \tag{A.2}$$

The power of RES generation is limited by the availability of the corresponding renewable resource (wind or sun):

$$o_{g,t}\underline{p}_g \leq p_{g,t} \leq o_{g,t}p^{\text{res}}_{g,t}, \quad g\in\mathcal{G}^{\text{res}}. \tag{A.3}$$

Unit on/off constraints: A unit can only be turned on if and only if it is in off state and vice versa:

$$u_{g,t} - d_{g,t} = o_{g,t} - o_{g,t-1}, \quad t\neq 1,\ g\in\mathcal{G}^{\text{syn}}. \tag{A.4}$$

In a rolling horizon approach, consistency between adjacent time slots is ensured by:

$$u_{g,t} - d_{g,t} = o_{g,t} - \hat{o}_g, \quad t = 1,\ g\in\mathcal{G}^{\text{syn}}, \tag{A.5}$$

Eqs. (A.4) and (A.5) also implicitly determine the upper bound of $u_{g,t}$ and $d_{g,t}$ in terms of changes in $o_{g,t}$.

Number of online units: An explicit upper bound on status variables, that is limited by maximum number of identical units at each generation station:

$$o_{g,t} \leq \overline{U}_g. \tag{A.6}$$

Ramp-up and ramp-down limits: Ramp rates of synchronous generation should be kept within the respective ramp-up (A.7), (A.8) and ramp-down limits (A.9), (A.10):

$$p_{g,t} - p_{g,t-1} \leq o_{g,t}r^+_g, \qquad t\neq 1, g\in\{\mathcal{G}^{\text{syn}}|r^+_g < \overline{p}_g\}, \tag{A.7}$$

$$p_{g,t} - \hat{p}_g \leq o_{g,t}r^+_g, \qquad t = 1, g\in\{\mathcal{G}^{\text{syn}}|r^+_g < \overline{p}_g\}, \tag{A.8}$$

$$\hat{p}_g - p_{g,t} \leq o_{g,t-1} r_g^-, \qquad t \neq 1, g \in \{\mathcal{G}^{\text{syn}} | r_g^- < \overline{p}_g\}, \tag{A.9}$$

$$\hat{p}_g - p_{g,t} \leq \hat{o}_g r_g^-, \qquad t = 1, g \in \{\mathcal{G}^{\text{syn}} | r_g^- < \overline{p}_g\}. \tag{A.10}$$

Minimum up and down times: Thermal generators must remain on for a period of time τ_g^{u} once turned on (minimum up time):

$$o_{g,t} \geq \sum_{\tilde{t}=\tau_g^{\text{u}}-1}^{0} u_{g,t-\tilde{t}}, \qquad t \geq \tau_g^{\text{u}},\ g \in \{\mathcal{G}^{\text{syn}} | \tau_g^{\text{u}} > \Delta t\}, \tag{A.11}$$

$$o_{g,t} \geq \sum_{\tilde{t}=t-1}^{0} u_{g,t-\tilde{t}} + \hat{u}_{g,t}, \qquad t < \tau_g^{\text{u}},\ g \in \{\mathcal{G}^{\text{syn}} | \tau_g^{\text{u}} > \Delta t\}. \tag{A.12}$$

Similarly, they must not be turned on for a period of time τ_g^{d} once turned off (minimum down time):

$$o_{g,t} \leq \overline{U}_g - \sum_{\tilde{t}=\tau_g^{\text{d}}-1}^{0} d_{g,t-\tilde{t}}, \qquad t \geq \tau_g^{\text{d}},\ g \in \{\mathcal{G}^{\text{syn}} | \tau_g^{\text{d}} > \Delta t\}, \tag{A.13}$$

$$o_{g,t} \leq \overline{U}_g - \sum_{\tilde{t}=t-1}^{0} d_{g,t-\tilde{t}} - \hat{d}_{g,t}, \qquad t < \tau_g^{\text{d}},\ g \in \{\mathcal{G}^{\text{syn}} | \tau_g^{\text{d}} > \Delta t\}. \tag{A.14}$$

Line power constraints: DC power flow formulation

$$p_{l,t}^{x,y} = B_l(\delta_{x,t} - \delta_{y,t}), \quad l \in \mathcal{L}^{\text{ac}}, \tag{A.15}$$

where the variables $\delta_{x,t}$ and $\delta_{y,t}$ represent voltage angles at nodes $x \in \mathcal{N}$ and $y \in \mathcal{N}$, respectively.

Thermal line limits: Power flows on all transmission lines are limited by the respective thermal limits of line l:

$$| p_{l,t} | \leq \overline{p}_l, \tag{A.16}$$

where $\overline{p}_l$ represents the thermal limit of line l.

Appendix B. Lower-level KKT optimality conditions

To ensure completeness, the full set of KKT optimality conditions is derived for the lower-level prosumer VPP optimization problem. The equality and inequality constraints of the lower-level, as represented by (13)–(15e), are reorganized and rewritten with the corresponding Lagrange multipliers indicated in parentheses:

$$p_{p,t}^{\text{g+}} + p_{p,t}^{\text{pv}} + p_{p,t}^{\text{LL,b}-} - p_{p,t}^{\text{d}} - p_{p,t}^{\text{LL,b+}} = 0, \qquad (\lambda_{p,t}^{\text{g+}}) \tag{B.1}$$

$$e_{p,t}^{\text{LL,b}} - e_{p,t-1}^{\text{LL,b}} - \eta_p^{\text{b+}} p_{p,t}^{\text{LL,b+}} + \frac{1}{\eta_p^{\text{b}-}} p_{p,t}^{\text{LL,b}-} = 0, \qquad (\lambda_{p,t}^{\text{e}}) \tag{B.2}$$

$$e_{p,t}^{\text{LL,b}} - \hat{e}_p^{\text{LL,b}} - \eta_p^{\text{b+}} p_{p,t}^{\text{LL,b+}} + \frac{1}{\eta_p^{\text{b}-}} p_{p,t}^{\text{LL,b}-} = 0, \qquad (\lambda_p^{\text{e}}) \tag{B.3}$$

$$p_{p,t}^{\text{pv}} - p_{p,t}^{\text{pv,total}} + p_{p,t}^{\text{curt}} = 0, \qquad (\lambda_{p,t}^{\text{pv}}) \tag{B.4}$$

$$-\, p_{p,t}^{\text{g+}} \leq 0, \qquad (\mu_{p,t}^{\text{g+}}) \tag{B.5}$$

$$-\, p_{p,t}^{\text{pv}} \leq 0, \qquad (\mu_{p,t}^{\text{pv}}) \tag{B.6}$$

$$-\, p_{p,t}^{\text{curt}} \leq 0, \qquad (\mu_{p,t}^{\text{curt}}) \tag{B.7}$$

$$\underline{e}_p^{\text{b}} - e_{p,t}^{\text{LL,b}} \leq 0, \qquad (\underline{\mu}_{p,t}^{\text{e}}) \tag{B.8}$$

$$e_{p,t}^{\text{LL,b}} - \overline{e}_p^{\text{b}} \leq 0, \qquad (\overline{\mu}_{p,t}^{\text{e}}) \tag{B.9}$$

$$-\, p_{p,t}^{\text{LL,b+}} \leq 0, \qquad (\underline{\mu}_{p,t}^{\text{b+}}) \tag{B.10}$$

$$p_{p,t}^{\text{LL,b+}} - r^{\text{b+}} \overline{e}_p^{\text{b}} \leq 0, \qquad (\overline{\mu}_{p,t}^{\text{p+}}) \tag{B.11}$$

$$-\, p_{p,t}^{\text{LL,b}-} \leq 0, \qquad (\underline{\mu}_{p,t}^{\text{p}-}) \tag{B.12}$$

$$p_{p,t}^{\text{LL,b}-} - r^{\text{b}-} \overline{e}_p^{\text{b}} \leq 0, \qquad (\overline{\mu}_{p,t}^{\text{p}-}) \tag{B.13}$$

The KKT conditions for the lower-level optimization problem are derived by first formulating the corresponding Lagrangian function:

$$\mathcal{L}(\mathbf{x}, \lambda, \boldsymbol{\mu}) = f(\mathbf{x}) + \lambda^\top \mathbf{g}(\mathbf{x}) + \boldsymbol{\mu}^\top \mathbf{h}(\mathbf{x}), \tag{B.14}$$

where $\mathbf{x} = \{p_{p,t}^{\text{g+}}, p_{p,t}^{\text{pv}}, p_{p,t}^{\text{curt}}, p_{p,t}^{\text{LL,b+}}, p_{p,t}^{\text{LL,b}-}, e_{p,t}^{\text{b}}\}$ represents the decision vector of the lower-level problem. The function $f(\mathbf{x})$ denotes the objective function (12), $\mathbf{g}(\mathbf{x})$ is the vector of equality constraints (B.1)–(B.4), and $\mathbf{h}(\mathbf{x})$ is the vector of inequality constraints (B.5)–(B.13). The vector of Lagrange multipliers associated with the equality constraints is given by $\lambda^\top = \{\lambda_{p,t}^{\text{g+}}, \lambda_{p,t}^{\text{e}}, \lambda_{p,t}^{\text{pv}}\}$, and the multipliers corresponding to the inequality constraints are represented as $\boldsymbol{\mu}^\top = \{\mu_{p,t}^{\text{g+}}, \mu_{p,t}^{\text{pv}}, \mu_{p,t}^{\text{curt}}, \underline{\mu}_{p,t}^{\text{e}}, \overline{\mu}_{p,t}^{\text{e}}, \underline{\mu}_{p,t}^{\text{b+}}, \overline{\mu}_{p,t}^{\text{p+}}, \underline{\mu}_{p,t}^{\text{p}-}, \overline{\mu}_{p,t}^{\text{p}-}\}$.

Following this, the KKT optimality conditions can be derived by first taking the derivative of the lower-level problem's Lagrangian function $\mathcal{L}$ with respect to its primal variables $\mathbf{x}$. This results in the introduction of the equality conditions given by constraints (B.15)–(B.21).

$$\frac{\partial \mathcal{L}}{\partial p_{p,t}^{\text{g+}}} = 1 + \lambda_{p,t}^{\text{g+}} - \mu_{p,t}^{\text{g+}} = 0, \tag{B.15}$$

$$\frac{\partial \mathcal{L}}{\partial p_{p,t}^{\text{pv}}} = \lambda_{p,t}^{\text{g+}} + \lambda_{p,t}^{\text{pv}} - \mu_{p,t}^{\text{pv}} = 0, \tag{B.16}$$

$$\frac{\partial \mathcal{L}}{\partial p_{p,t}^{\text{curt}}} = \lambda_{p,t}^{\text{pv}} - \mu_{p,t}^{\text{curt}} = 0, \tag{B.17}$$

$$\frac{\partial \mathcal{L}}{\partial p_{p,t}^{\text{LL,b+}}} = c_{p,t}^{\text{pen}} - \lambda_{p,t}^{\text{g+}} - \eta_p^{\text{b+}} \lambda_{p,t}^{\text{e}} + \overline{\mu}_{p,t}^{\text{b+}} - \underline{\mu}_{p,t}^{\text{b+}} = 0, \tag{B.18}$$

$$\frac{\partial \mathcal{L}}{\partial p_{p,t}^{\text{LL,b}-}} = c_{p,t}^{\text{pen}} + \lambda_{p,t}^{\text{g+}} + \frac{1}{\eta_p^{\text{b}-}} \lambda_{p,t}^{\text{e}} + \overline{\mu}_{p,t}^{\text{b}-} - \underline{\mu}_{p,t}^{\text{b}-} = 0, \tag{B.19}$$

$$\frac{\partial \mathcal{L}}{\partial e_{p,t}^{\text{LL,b}}} = \lambda_{p,t}^{\text{e}} - \lambda_{p,t+1}^{\text{e}} + \overline{\mu}_{p,t}^{\text{e}} - \underline{\mu}_{p,t}^{\text{e}} = 0, \quad t < T \tag{B.20}$$

$$\frac{\partial \mathcal{L}}{\partial e_{\text{p}}^{\text{LL,b}}} = \lambda_{p,T}^{\text{e}} + \overline{\mu}_{p,T}^{\text{e}} - \underline{\mu}_{p,T}^{\text{e}} = 0, \qquad t = T \tag{B.21}$$

Second, the equality constraints of the primal lower-level problem are given by (B.1)–(B.4). Finally, the complementarity conditions related to the inequality constraints are given as follows:

$$0 \leq h(\mathbf{x}) \perp \mu \geq 0, \tag{B.22a}$$

where $h(\mathbf{x})$ represents the inequality constraints (B.5)–(B.13); μ denotes the Lagrange multiplier associated with each inequality constraint. These complementarity constraints are then linearized using the well-known Big-M approach. Each constraint of the form $0 \leq h(x) \perp \mu \geq 0$ is replaced by:

$$h(\mathbf{x}) \geq 0, \qquad \mu \geq 0, \tag{B.23a}$$

$$h(\mathbf{x}) \leq bM, \quad \mu \leq (1-b)M, \tag{B.23b}$$

where M is a sufficiently large number, and b is a binary decision variable.

Given that the KKT conditions are both sufficient and necessary for optimality, the lower-level problem (12)–(15e) can be replaced with mixed integer linear constraints (B.15)–(B.21), (B.1)–(B.4), and (B.23a) and (B.23b).

Hence, the production cost model is structured as a MILP that can be solved efficiently with off-the-shelf solvers described by the following:

objective (2)

subject to

(3)–(11), (A.1)–(A.16),(B.1)–(B.4), (B.15)–(B.21),

(B.23a) and (B.23b).

where the decision variables are Ω, Ω_p, λ, μ, and b.

Appendix C. Supplementary data

Supplementary material related to this article can be found online at github.com/mald1409/Capacity-Firming-Data.

References

[1] World energy transitions outlook: 1.5°c pathway. Tech. rep., International Renewable Energy Agency (IRENA); 2021.

[2] Integrated system plan. Tech. rep., Australian Energy Market Operator (AEMO); 2024.

[3] McDonnell M, Gorman J, Kahrl F, Kristov L, Keeling J, Sreedharan P. DER integration into wholesale markets and operations. Tech. rep., Energy Systems Integration Group (ESIG), Distributed Energy Resources Task Force; 2022.

[4] Valuing load flexibility in the NEM. Tech. rep., Australian Renewable Energy Agency (ARENA); 2022.

[5] Denholm P, Hand M. Grid flexibility and storage required to achieve very high penetration of variable renewable electricity. Energy Policy 2011;39(3):1817–30. http://dx.doi.org/10.1016/j.enpol.2011.01.019.

[6] Moving to a two-sided market. Tech. rep., Energy Security Board (ESB); 2020.

[7] Consumer energy resources and the transformation of the NEM. Tech. rep., Energy Security Board (ESB); 2024.

[8] Projections for small-scale embedded technologies. Tech. rep., Graham, Paul and Havas, Lisa: CSIRO, Australia; 2020.

[9] Gilmore J, Nelson T, Nolan T. Firming technologies to reach 100% renewable energy production in Australia's national electricity market (NEM). Energy J 2023;44(01). http://dx.doi.org/10.5547/01956574.44.6.jgil.

[10] Flottmann JH, Akimov A, Simshauser P. Firming merchant renewable generators in Australia's National Electricity Market. Econ Anal Policy 2022;74:262–76. http://dx.doi.org/10.1016/j.eap.2022.02.005.

[11] Beltran H, Cardo-Miota J, Segarra-Tamarit J, Pérez E. Battery size determination for photovoltaic capacity firming using deep learning irradiance forecasts. J Energy Storage 2021;33:102036. http://dx.doi.org/10.1016/j.est.2020.102036.

[12] Dumas J, Cointe C, Wehenkel A, Sutera A, Fettweis X, Cornélusse B. A probabilistic forecast-driven strategy for a risk-aware participation in the capacity firming market. IEEE Trans Sustain Energy 2022;13(2):1234–43. http://dx.doi.org/10.1109/TSTE.2021.3117594.

[13] Bucksteeg M. Modelling the impact of geographical diversification of wind turbines on the required firm capacity in Germany. Appl Energy 2019;235:1476–91. http://dx.doi.org/10.1016/j.apenergy.2018.11.031.

[14] Campaigne C, Oren SS. Firming renewable power with demand response: an end-to-end aggregator business model. J Regul Econ 2016;50(1):1–37. http://dx.doi.org/10.1007/s11149-016-9301-y.

[15] Freire-Barceló T, Martín-Martínez F, Rivier M, Sánchez-Miralles, San Román TG, Huclin S, et al. Storage and demand response contribution to firm capacity: Analysis of the Spanish electricity system. Energy Rep 2022;8:10546–60. http://dx.doi.org/10.1016/j.egyr.2022.08.014.

[16] Göke L, Weibezahn J, Kendziorski M. How flexible electrification can integrate fluctuating renewables. Energy 2023;278:127832. http://dx.doi.org/10.1016/j.energy.2023.127832.

[17] Pantoš M, Riaz S, Chapman AC, Verbič G. Capacity firming of intermittent generation by dispersed energy storage. In: 2017 Australasian universities power engineering conference (AUPEC). 2017, http://dx.doi.org/10.1109/AUPEC.2017.8282510.

[18] Brinkman G, Bain D, Buster G, Draxl C, Das P, Ho J, et al. The North American renewable integration study (NARIS): a U.S. Perspective. Tech. rep. NREL/TP-6A20-79224, National Renewable Energy Laboratory (NREL); 2021, http://dx.doi.org/10.2172/1804701.

[19] ENTSOG TYNDP 2024 scenarios methodology report. Tech. rep., ENTSO-e; 2024.

[20] Denholm P, Arent DJ, Baldwin SF, Bilello DE, Brinkman GL, Cochran JM, et al. The challenges of achieving a 100% renewable electricity system in the United States. Joule 2021;5(6):1331–52. http://dx.doi.org/10.1016/j.joule.2021.03.028.

[21] Barrows C, Hummon M, Jones W, Hale E. Time domain partitioning of electricity production cost simulations. Tech. rep. NREL/TP–6A20-60969, National Renewable Energy Laboratory (NREL); 2014, http://dx.doi.org/10.2172/1123223.

[22] Diakov V, Cole W, Sullivan P, Brinkman G, Margolis R. Improving power system modeling. A tool to link capacity expansion and production cost models. Tech. rep. NREL/TP–6A20-64905, 2015, http://dx.doi.org/10.2172/1233204.

[23] Apablaza P, Püschel-Løvengreen S, Moreno R, Mhanna S, Mancarella P. Assessing the impact of DER on the expansion of low-carbon power systems under deep uncertainty. Electr Power Syst Res 2024;235. http://dx.doi.org/10.1016/j.epsr.2024.110824.

[24] Conejo AJ, Ruiz C. Complementarity, not optimization, is the language of markets. IEEE Open Access J Power Energy 2020;7:344–53. http://dx.doi.org/10.1109/OAJPE.2020.3029134.

[25] Guo H, Chen Q, Shahidehpour M, Xia Q, Kang C. Bidding behaviors of GENCOs under bounded rationality with renewable energy. Energy 2022;250:123793. http://dx.doi.org/10.1016/j.energy.2022.123793.

[26] Vayá MGonzález, Andersson G. Optimal bidding strategy of a plug-in electric vehicle aggregator in day-ahead electricity markets under uncertainty. IEEE Trans Power Syst 2015;30(5):2375–85. http://dx.doi.org/10.1109/TPWRS.2014.2363159.

[27] Wang P, Guo Z, Zhang S, Zhu L, Yi L, Song X. Strategic behaviors of renewable energy generation companies participating in the electricity and carbon coupled markets based on non-cooperative game theory. Energy 2024;312:133522. http://dx.doi.org/10.1016/j.energy.2024.133522.

[28] Dimitriadis CN, Tsimopoulos EG, Georgiadis MC. Strategic bidding of an energy storage agent in a joint energy and reserve market under stochastic generation. Energy 2022;242:123026. http://dx.doi.org/10.1016/j.energy.2021.123026.

[29] Asimakopoulou GE, Vlachos AG, Hatziargyriou ND. Hierarchical decision making for aggregated energy management of distributed resources. IEEE Trans Power Syst 2015;30(6):3255–64. http://dx.doi.org/10.1109/TPWRS.2015.2390412.

[30] Raja SC, Kumar NMV, kumar JS, Nesamalar JJD. Enhancing system reliability by optimally integrating PHEV charging station and renewable distributed generators: A Bi-Level programming approach. Energy 2021;229:120746. http://dx.doi.org/10.1016/j.energy.2021.120746.

[31] Zugno M, Morales JM, Pinson P, Madsen H. A bilevel model for electricity retailers' participation in a demand response market environment. Energy Econ 2013;36:182–97. http://dx.doi.org/10.1016/j.eneco.2012.12.010.

[32] Riaz S, Marzooghi H, Verbič G, Chapman AC, Hill DJ. Generic demand model considering the impact of prosumers for future grid scenario analysis. IEEE Trans Smart Grid 2019;10(1):819–29. http://dx.doi.org/10.1109/TSG.2017.2752712.

[33] Palmintier BS, Webster MD. Heterogeneous unit clustering for efficient operational flexibility modeling. IEEE Trans Power Syst 2014;29(3):1089–98. http://dx.doi.org/10.1109/TPWRS.2013.2293127.

[34] Distributed energy integration program (DEIP), dynamic operating envelopes workstream: outcomes report. Tech. rep., Australian Renewable Energy Agency (ARENA); 2022.

[35] Wu Q, Li C. A bi-level optimization framework for the power-side virtual power plant participating in day-ahead wholesale market as a price-maker considering uncertainty. Energy 2024;304:132050. http://dx.doi.org/10.1016/j.energy.2024.132050.

[36] Gjorgievski VZ, Cundeva S, Markovska N, Georghiou GE. Virtual net-billing: A fair energy sharing method for collective self-consumption. Energy 2022;254:124246. http://dx.doi.org/10.1016/j.energy.2022.124246.

[37] Yu H, Xu F, Chen C, Chen Y, Zhang W, Yang L, et al. Asymmetric nash bargaining-based community-centric energy sharing strategy for numerous prosumers. Energy 2025;316:134468. http://dx.doi.org/10.1016/j.energy.2025.134468.

[38] Golmaryami S, Nunes ML, Ferreira P. The role of social learning on consumers' willingness to engage in demand-side management: An agent-based modelling approach. Smart Energy 2024;14:100138. http://dx.doi.org/10.1016/j.segy.2024.100138.

[39] Pelka S, Kesselring A, Preuß S, Chappin E, De Vries L. Can behavioral interventions optimize self-consumption? Evidence from a field experiment with prosumers in Germany. Smart Energy 2024;14:100140. http://dx.doi.org/10.1016/j.segy.2024.100140.

[40] Thompson AW. Economic implications of lithium ion battery degradation for Vehicle-to-Grid (V2X) services. J Power Sources 2018;396:691–709. http://dx.doi.org/10.1016/j.jpowsour.2018.06.053.

[41] Morstyn T, Hredzak B, Aguilera RP, Agelidis VG. Model predictive control for distributed microgrid battery energy storage systems. IEEE Trans Control Syst Technol 2018;26(3):1107–14. http://dx.doi.org/10.1109/TCST.2017.2699159.

[42] Gibbard M, Vowles D. Simplified 14-generator model of the SE Australian power system. Tech. rep., The University of Adelaide; 2010.

[43] Nagrath K. Agl's plan to replace liddell is cheaper and cleaner than keeping it open. Converstaion 2018. URL theconversation.com/agls-plan-to-replace-liddell-is-cheaper-and-cleaner-than-keeping-it-open-94651.

[44] 2012 NTNDP assumptions and inputs. Tech. rep., Australian Energy Market Operator (AEMO); 2012.

[45] Downing SD, Socie DF. Simple rainflow counting algorithms. Int J Fatigue 1982;4(1):31–40. http://dx.doi.org/10.1016/0142-1123(82)90018-4.

[46] Xu B, Oudalov A, Ulbig A, Andersson G, Kirschen DS. Modeling of lithium-ion battery degradation for cell life assessment. IEEE Trans Smart Grid 2018;9(2):1131–40. http://dx.doi.org/10.1109/TSG.2016.2578950.

[47] Xu B, Zhao J, Zheng T, Litvinov E, Kirschen DS. Factoring the cycle aging cost of batteries participating in electricity markets. IEEE Trans Power Syst 2018;33(2):2248–59. http://dx.doi.org/10.1109/TPWRS.2017.2733339.

[48] PowerTech Advanced Energy Storage Systems. Lithium iron phosphate (LFP or LiFePO4). 2025, URL www.powertechsystems.eu/home/tech-corner/lithium-iron-phosphate-lifepo4/. Accessed on 10 March 2025.

[49] Eco Lithium Battery Energy Group. Which is better? Lithium titanate battery or lithium iron phosphate?. 2025, URL www.ecolithiumbattery.com/lithium-titanate-battery/. Accessed on 10 March 2025.

[50] Khafaf NAl, Rezaei AA, Amani AMoradi, Jalili M, McGrath B, Meegahapola L, et al. Impact of battery storage on residential energy consumption: An Australian case study based on smart meter data. Renew Energy 2022;182:390–400. http://dx.doi.org/10.1016/j.renene.2021.10.005.

[51] Lai X, Gu H, Chen Q, Tang X, Zhou Y, Gao F, et al. Investigating greenhouse gas emissions and environmental impacts from the production of lithium-ion batteries in China. J Clean Prod 2022;372:133756. http://dx.doi.org/10.1016/j.jclepro.2022.133756.

[52] Han S, Zhenghao M, Meilin L, Xiaohui Y, Xiaoxue W. Global supply sustainability assessment of critical metals for clean energy technology. Resour Policy 2023;85:103994. http://dx.doi.org/10.1016/j.resourpol.2023.103994.

[53] Quinet P, Proost J, Lierde AV. Recovery of precious metals from electronic scrap by hydrometallurgical processing routes. Min Met Explor 2005;22:17–22. http://dx.doi.org/10.1007/BF03403191.

[54] Xu P, et al. Efficient direct recycling of lithium-ion battery cathodes by targeted healing. Joule 2020;4(12):2609–26. http://dx.doi.org/10.1016/j.joule.2020.10.008.

[55] Rinne M, Lappalainen H, Lundström M. Evaluating the possibilities and limitations of the pyrometallurgical recycling of waste li-ion batteries using simulation and life cycle assessment. Green Chem 2025. http://dx.doi.org/10.1039/D4GC05409A, –.

[56] Zhou H, et al. Eu's recycled content targets of lithium-ion batteries are likely to compromise critical metal circularity. One Earth 2024;7(7):1288–300. http://dx.doi.org/10.1016/j.oneear.2024.06.012.

[57] Yan Z, Zhao L, Wang Y, Zhu Z, Chou S. The future for room-temperature sodium–sulfur batteries: From persisting issues to promising solutions and practical applications. Adv Funct Mater 2022;32(36):2205622. http://dx.doi.org/10.1002/adfm.202205622.

[58] Fallah N, Fitzpatrick C. How will retired electric vehicle batteries perform in grid-based second-life applications? A comparative techno-economic evaluation of used batteries in different scenarios. J Clean Prod 2022;361:132281. http://dx.doi.org/10.1016/j.jclepro.2022.132281.

[59] Baars J, Domenech T, Bleischwitz R, Melin HE, Heidrich O. Circular economy strategies for electric vehicle batteries reduce reliance on raw materials. Nat Sustain 2021;4(1):71–9. http://dx.doi.org/10.1038/s41893-020-00607-0.

[60] Lander L, Tagnon C, Nguyen-Tien V, Kendrick E, Elliott RJ, Abbott AP, et al. Breaking it down: A techno-economic assessment of the impact of battery pack design on disassembly costs. Appl Energy 2023;331:120437. http://dx.doi.org/10.1016/j.apenergy.2022.120437.

[61] Wang B, Verbič G. Stability analysis of low-voltage distribution feeders operated as islanded microgrids. IEEE Trans Smart Grid 2021;12(6):4681–9. http://dx.doi.org/10.1109/TSG.2021.3103530.